INTRAMEMBRANE ORGANIZATION OF SPECIALIZED CONTACTS IN THE OUTER PLEXIFORM LAYER OF THE RETINA

A Freeze-Fracture Study in Monkeys and Rabbits

ELIO RAVIOLA and NORTON B. GILULA

From the Department of Anatomy, Harvard Medical School, Boston, Massachusetts 02115, and The Rockefeller University, New York 10021

ABSTRACT

Freeze-fracture analysis of the neural connections in the outer plexiform layer of the retina of primates (*Macaca mulatta* and *Macaca arctoides*) demonstrates a remarkable diversity in the internal structure of the synaptic membranes. In the invaginating synapses of cone pedicles, the plasma membrane of the photoreceptor ending contains an aggregate of A-face particles, a hexagonal array of synaptic vesicle sites, and rows of coated vesicle sites, which are deployed in sequence from apex to base of the synaptic ridge. The horizontal cell dendrites lack vesicle sites and have two aggregates of intramembrane A-face particles, one at the interface with the apex of the synaptic ridge, the other opposite the tip of the invaginating midget bipolar dendrite. Furthermore, the horizontal cell dendrites are interconnected by a novel type of specialized junction, characterized by: (*a*) enlarged intercellular cleft, bisected by a dense plate and traversed by uniformly spaced crossbars; (*b*) symmetrical arrays of B-face particles arranged in parallel rows within the junctional membranes; and (*c*) a layer of dense material on the cytoplasmic surface of the membranes. The plasmalemma of the invaginating midget bipolar dendrite is unspecialized. At the contact region between the basal surface of cone pedicles and the dendrites of the flat midget and diffuse cone bipolar cells, the pedicle membrane has moderately clustered A-face particles, but no vesicle sites, whereas the adjoining membrane of the bipolar dendrites contains an aggregate of B-face particles. The invaginating synapse of rod spherules differs from that of cone pedicles, because the membrane of the axonal endings of the horizontal cells only has an A-face particle aggregate opposite the apex of the synaptic ridge. Specialized junctions between horizontal cell processes, characterized by symmetrical arrays of intramembrane B-face particles, are also present in the neuropil underlying the photoreceptor endings. Small gap junctions connect the processes of the horizontal cells; other gap junctions probably connect the bipolar cell dendrites which make contact with each cone pedicle. Most of the junctional specializations typical of the primate outer plexiform layer are also found in the

rabbit retina. The fact that specialized contacts between different types of neurons interacting in the outer plexiform layer have specific arrangements of intramembrane particles strongly suggests that the internal structure of the synaptic membranes is intimately correlated with synaptic function.

The outer plexiform layer of the retina is the region of synaptic interplay between photoreceptor, bipolar, and horizontal cells. In primates, the interneuronal connections of this layer have been studied in great detail with both the chromo-argentic impregnation and electron microscopy of thin-sectioned retinas (4, 5, 12, 23, 29, 40). Cone cells synapse with the dendrites of horizontal cells and the dendrites of three varieties of bipolar cells: invaginating midget, flat midget, and diffuse cone bipolar cells. Rod cells synapse with the axonal endings of horizontal cells and the dendrites of the rod bipolar cells. The synaptic ending of a cone cell or pedicle makes both invaginating and basal synapses. Each synaptic invagination contains a precise geometrical arrangement of two dendrites from the horizontal cells and one dendrite from an invaginating midget bipolar cell. Basal synapses, in turn, are specialized contacts between the vitreal surface of the pedicle and the dendrites of the flat midget and diffuse cone bipolar cells. The synaptic nature of these basal contacts has been inferred from the fact that they represent the only site of surface apposition between photoreceptor and flat midget or diffuse cone bipolars. The synaptic endings of rod cells or spherules have a single synaptic invagination and no basal contacts. The invaginating synapse of rod spherules contains the extremity of two axonal branchlets of the horizontal cells and a variable number of dendrites which belong to the rod bipolar cells.

Thus, the primate retina is perfectly suited for a morphological analysis of the synapses in the outer plexiform layer for several reasons: (*a*) the parent neurons of the processes interacting at the synapses are identified; (*b*) the synapsing processes are extremely consistent in shape and mutual arrangement; and (*c*), finally, because the pedicle and spherule synapses represent the only site of specialized contact between photoreceptor, bipolar, and horizontal cells. However, in spite of the considerable amount of information on the connectivity of this layer, no conclusions can yet be made about neural interaction at the synapses, for the structural polarity of the contacts is ambiguous and the distal retinal neurons in primates have not been successfully examined with microelectrodes.

In the present study, the internal structure of the membrane at specialized neural contacts in the outer plexiform layer of the primate retina was investigated with the freeze-fracturing technique (31), which splits cell membranes and thus exposes their internal structure (6, 39, 52). A large variety of intramembrane specializations is described at the interface between photoreceptor, bipolar, and horizontal cells; some of the existing uncertainties on the connectivity of the outer plexiform layer are resolved, and a new dimension of complexity is introduced in the structural analysis of interneuronal synapses. In addition, the rabbit has been examined to determine whether the membrane specializations observed in primates are typical of the mammalian retina in general. A preliminary account of this study has been presented elsewhere in abstract form (42).

MATERIALS AND METHODS

Adult monkeys (*Macaca mulatta* and *Macaca arctoides*) and rabbits (New Zealand albino and Dutch belted) were used. The eye globe was dissected from pentobarbital-anesthetized animals and opened with an equatorial incision. The vitreous body was removed from the posterior hemisphere and the eye cup was immersed in the fixative fluid. The whole procedure was performed under normal room illumination. Two fixation methods were used: (*a*) 20-min immersion at room temperature in a solution containing 2% formaldehyde, 2.5% glutaraldehyde, 0.4% $CaCl_2$ in 0.07 M cacodylate buffer at pH 7.4 (21); and (*b*) 10-min immersion at room temperature in a solution containing 0.75% formaldehyde, 1% sucrose, and 0.4% $CaCl_2$ in 0.07 M cacodylate buffer at pH 7.4 (17), followed by a 10-min immersion in fixative (*a*). Specimens were subsequently rinsed for 30 min in 0.1 M cacodylate buffer at pH 7.4 containing 0.4% $CaCl_2$. The sclera was removed and the remaining ocular tunics trimmed and equilibrated with 20% glycerol in 0.1 M cacodylate buffer (pH 7.4) for 2 h at room temperature. In monkeys, the fovea, the rest of the central area (defined as the region encircled by large blood vessels), and the retinal periphery were processed separately. The retina, with the choroid still attached, was mounted perpendicularly on cardboard disks, rapidly frozen in the liquid phase of partially solidified Freon 22 (monochlorodifluoromethane), and stored in liquid nitrogen. The specimens were fractured at −115°C and replicated, without etching, in a Balzer's apparatus

(Balzer's High Vacuum Corp., Santa Ana, Calif.). The replicas were cleaned with methanol and bleach, mounted on unsupported grids, and examined with either a Jeolco 100 B or a Philips 300 electron microscope. For thin sectioning the retinas were fixed overnight in solution (*a*), rinsed in buffer, postfixed with 1% OsO_4 in 0.1 M cacodylate buffer (pH 7.4) containing 0.4% $CaCl_2$, stained *en bloc* with uranyl acetate in maleate buffer (21), and embedded in an Epon-Araldite mixture.

For the sake of brevity, the terms A-face and B-face particles are used here to indicate intramembrane particles which remain preferentially associated with the inner and, respectively, outer portion of the fractured plasmalemma. Illustrations are presented with the shadow direction approximately from bottom to top, and their orientation with respect to the layering of the retina is indicated by an arrow pointing in the direction of the vitreous body.

RESULTS

Monkey Retina. Thin-Sectioned Specimens

The outer plexiform layer consists of an outer zone formed by the photoreceptor inner fibers, a middle zone occupied by the photoreceptor synaptic endings, and an inner zone traversed by the branching processes of the bipolar and horizontal cells, which course from the cell body toward their synapses with the photoreceptor endings. The electron microscope organization of the layer is well understood (12, 23, 29); thus, the present description is concerned only with details of fine structure and patterns of neural interconnections in the middle and inner zones of the layer, which are useful for the interpretation of the freeze-fracture images.

CONE PEDICLE SYNAPSES: In each of the 12–25 invaginating synapses,[1] a deeply inserted dendrite from the horizontal cells lies on either side of a wedge-shaped projection of the cone pedicle, called the synaptic ridge. The dendritic terminal of an invaginating midget bipolar cell lies centrally and less deeply inserted; its tip is therefore separated from the apex of the synaptic ridge by a 40–120-nm long intercellular cleft, flanked on either side by the medial surface of the adjoining horizontal cell dendrites.

The synaptic ridge is bisected by a dense lamella or ribbon (48), surrounded by a halo of synaptic vesicles 40–45 nm in diameter (Figs. 1–3). Tenuous arms have been described connecting the ribbon to the vesicles (15), and sections parallel to the apex of the ridge demonstrate that the vesicles are aligned in rows at a center-to-center distance of 40–80 nm. The vesicle halo is incomplete at the apex of the ridge, for the edge of the ribbon is separated from the plasmalemma by a dense trough, the arciform density (24), whose geometric projection on the underlying membrane extends about 70 nm on either slope of the synaptic ridge. Thus, on both sides of the arciform density, a row of vesicles is commonly found wedged between ribbon, arciform density, and pedicle membrane; these vesicles are intimately applied to the plasmalemma and sometimes open into the intercellular cleft. The sites of interaction between vesicle membrane and plasmalemma are located at a distance of 100–150 nm from the apex of the synaptic ridge. Frequently, an additional row of vesicles lateral to the first one, and occasionally a third one contact the plasma membrane of the slopes of the ridge. At the apex of the ridge the pedicle membrane conforms in its course to the regular convexity of the underlying arciform density, but more laterally, it becomes undulated. Coated membrane invaginations are often associated with the pedicle plasmalemma at the bottom of the deep valleys on either side of the synaptic ridge.

The horizontal cell dendrites contain a small number of randomly distributed vesicles. Three regions can be distinguished on their medial surface: (*a*) at the interface with the synaptic ridge, the intercellular cleft enlarges to 15 nm and a layer of dense, fluffy material underlies the plasmalemma of the horizontal cell dendrite. This surface specialization extends for 100–250 nm, and therefore lies in register with both the arciform density and the adjoining row of vesicles in the synaptic ridge. (*b*) At the interface between adjoining horizontal cell dendrites, the intercellular cleft is 20–30 nm in width. It is bisected by a median plate and also bridged by a regular array of moderately dense crossbars (three to five in number), which are spaced 15 nm from each other. Fluffy material adheres to the inner aspect of the plasmalemma (Fig. 3). (*c*) At the interface between horizontal cell dendrites and the tip of the invaginating midget

[1] The invaginating synapse of cone pedicles in the monkey is a bilaterally symmetrical structure, the plane of symmetry being defined by the ribbon and the apex of the synaptic ridge. The terms median or central therefore define unpaired structures bisected by the plane of symmetry, such as the invaginating midget bipolar dendrite. Medial and lateral are used here in their classical anatomical sense to define the relative position of structures with respect to the plane of symmetry.

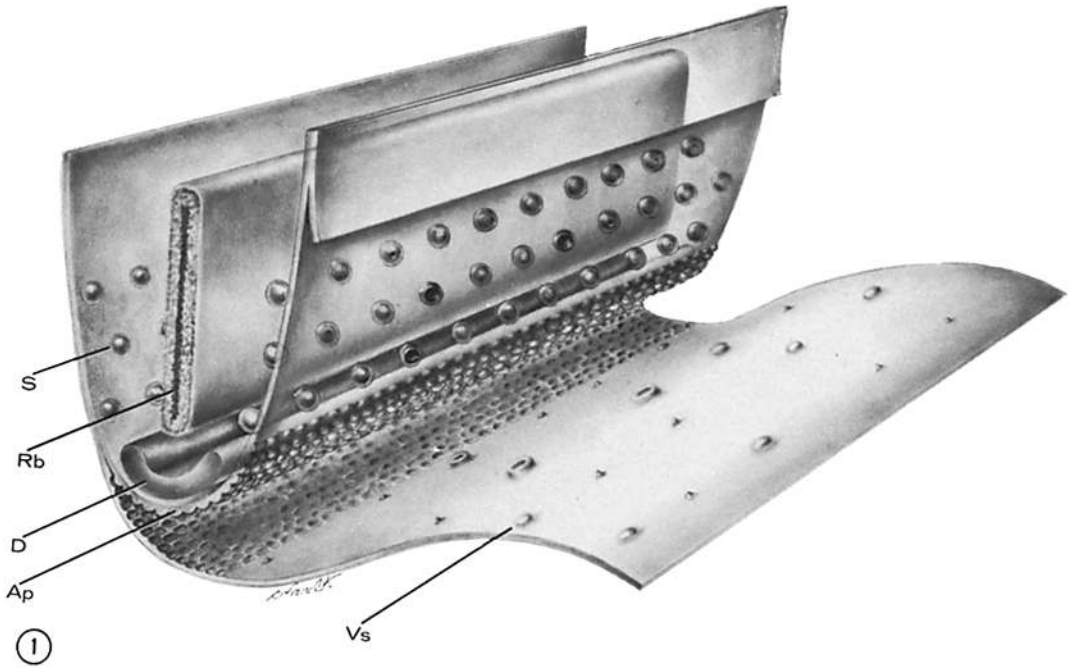

FIGURE 1 Diagram of the synaptic ridge in a photoreceptor cell ending. The synaptic ridge is bisected by a dense lamella or ribbon (*Rb*), separated from the plasma membrane by a trough-shaped arciform density (*D*). Synaptic vesicles (*S*) in an orderly hexagonal array are bound to the ribbon and positioned against the plasmalemma on the slopes of the ridge. Upon freeze-fracturing, the plasma membrane is split and its internal organization exposed. An aggregate of intramembrane particles is present at the apex of the ridge; they remain preferentially associated with the inner portion of the membrane (A face particles, *Ap*) and leave a complementary set of pits on the surface of the outer membrane portion (B face). On the slopes of the ridge, the B face of the pedicle membrane displays a hexagonal array of protrusions, which represent sites of interaction between vesicles and plasmalemma (synaptic vesicle sites, *Vs*).

bipolar dendrite, the adjoining membranes run closely parallel to each other, separated by a slightly enlarged intercellular cleft (10–12 nm), and the membrane of the horizontal cell dendrite is underlined by a layer of dense material (Fig. 3).

The membrane at the tip of the invaginating midget bipolar dendrite is unspecialized. However, at the neck of the synaptic invagination where the bipolar dendrite directly contacts the cone pedicle, both adjoining membranes may bear an undercoat of fluffy material.

The vitreal surface of the cone pedicles makes hundreds of specialized contacts with the dendrites of the flat midget and diffuse cone bipolars. These basal contacts occur at shallow indentations of the pedicle base. The adjoining cell membranes bear a coat of dense cytoplasmic material and run a parallel course, separated by a 13-nm intercellular cleft. In the pedicle cytoplasm neither ribbons nor vesicles are preferentially associated with the plasmalemma.

ROD SPHERULE SYNAPSE: In the invaginating synapse of rod spherules two deeply inserted endings of horizontal cell axons lie on either side of the synaptic ridge; one to four dendritic terminals of rod bipolar cells lie centrally and less deeply inserted. The synaptic ridge and the bipolar dendrites have the same appearance as in pedicle invaginating synapses. The horizontal cell endings consistently contain randomly dispersed vesicles and their membrane bears a layer of fluffy cytoplasmic material which lies opposite the synaptic ridge and in register with both the arciform density and the adjoining row of vesicles. However, in contrast to cone pedicles, neither the interface between the adjoining axonal endings of the horizontal cells nor the interface between these endings and the rod bipolar dendrites is specialized.

INNER ZONE OF THE OUTER PLEXIFORM LAYER: In the neuropil beneath the cone pedicles, desmosome-like specializations (Fig. 4) frequently occur between processes con-

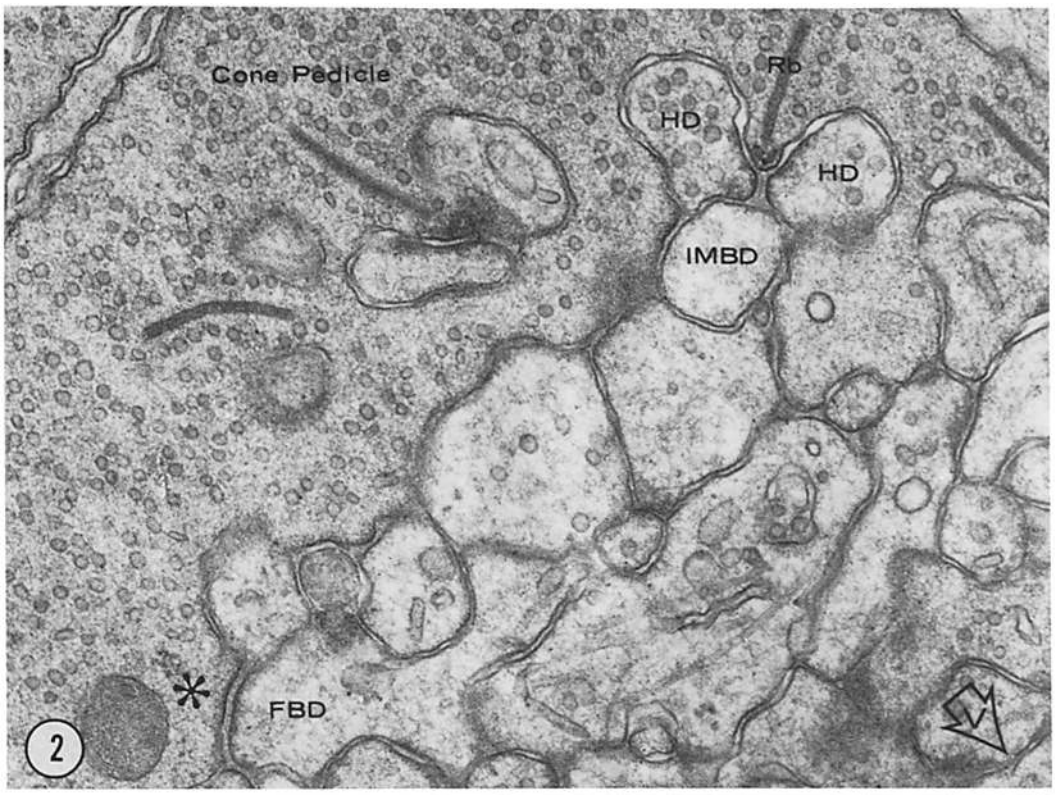
Cone Pedicle
Rb
HD
HD
IMBD
FBD
2

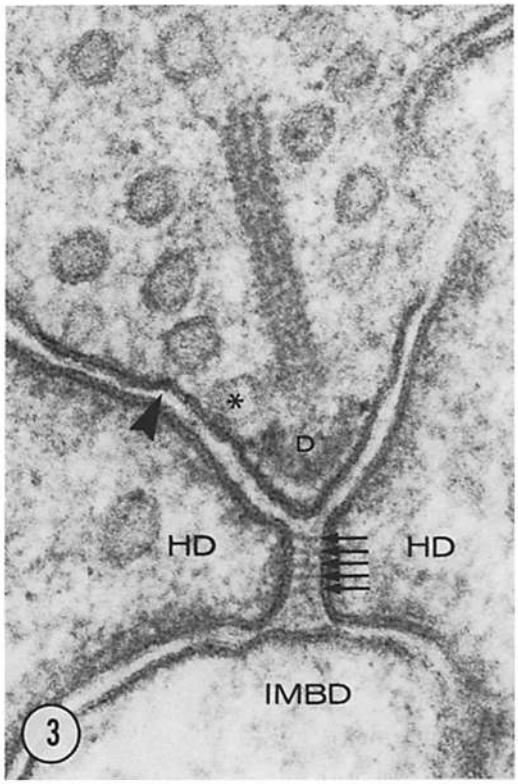
*
D
HD
HD
IMBD
3

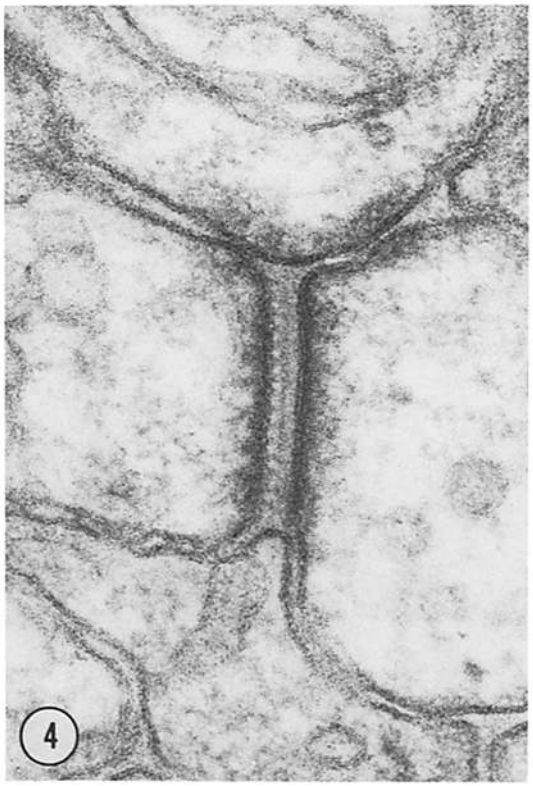
4

taining a small number of randomly dispersed vesicles (30). At high magnification, they closely resemble the specialized junction between adjoining horizontal cell dendrites in pedicle invaginating synapses: about 250 nm long, they are characterized by dense, fluffy material on the inner aspect of both adjoining membranes and by an intercellular cleft 20–30 nm wide. The intercellular cleft is bisected by a median plate and bridged by a regular array of crossbars spaced 15 nm from each other. In *Macaca arctoides* these specialized junctions are occasionally seen between processes rich in mitochondria, a feature typical of the dendrites and bodies of horizontal cells in this monkey species. They also join the body of horizontal cells to neighboring processes.

Monkey retina. Freeze-Fractured Specimens

The freeze-fracture replicas of the outer plexiform and nuclear layers contain a considerable amount of three dimensional information which permits positive identification of photoreceptor endings, horizontal and bipolar cells on the basis of their characteristic shape and topography (Fig. 5). The following description applies to both central and peripheral regions of the retina in *Macaca mulatta* and *Macaca arctoides*, for no significant regional or species differences are apparent in the organization of the junctional membranes.

CONE PEDICLES: On the lateral surface of cone pedicles the plasma membrane contains a rich complement of randomly distributed particles which are preferentially associated with the cytoplasmic portion of the fractured membrane (fracture face A). Linear arrays or homogeneous clusters of particles are also present, located on smooth bulges of the membrane A face; these components have been identified as the interreceptor gap junctions (43). Cross-fractured pedicles contain mitochondria and a population of spherical synaptic vesicles 40–45 nm in diameter; the particles in the vesicle membrane are associated with both the cytoplasmic and adluminal fracture faces. The synaptic ribbon and the underlying arciform density do not influence the course of the fracture process; thus, their chemical organization does not provide a preferential fracture plane. In slightly etched specimens, the ribbon can be recognized as a linear array of irregular protrusions emerging from the surrounding cytoplasmic matrix (Fig. 6 *a*).

When the retina is oriented perpendicularly to the cutting edge, freeze-fracturing the invaginating synapse produces three basic sets of images. (*a*) The fracture plane may pass perpendicularly through the synaptic ridge; in this instance the replica contains very little information on the internal organization of the synaptic membranes, and the resulting image closely conforms to the thin-sectioned appearance of the invaginating synapse. (*b*) The fracture plane may pass obliquely through the synaptic ridge; in this instance the replica provides a view of the A and B faces of the pedicle plasmalemma on either side of the obliquely fractured synaptic ridge. It also exposes the membrane A face on the medial surface of one horizontal cell dendrite and the membrane B face of the other one. In addition, it may reveal either the A or

FIGURE 2 *Macaca arctoides*, perifoveal cone pedicle. In the invaginating synapse, two deeply inserted horizontal cell dendrites (*HD*) lie on either side of the synaptic ridge, which is bisected by the ribbon (*Rb*). The dendritic terminal of an invaginating midget bipolar cell (*IMBD*) lies centrally, and less deeply inserted. A basal contact (asterisk) between the pedicle and a dendrite of a flat bipolar cell (*FBD*) is also present. The arrow labeled *V* points toward the vitreous body. × 30,000.

FIGURE 3 *Macaca arctoides*, perifoveal cone pedicle. In the synaptic ridge, the ribbon is separated from the plasmalemma by the arciform density (*D*). A synaptic vesicle (asterisk), wedged between ribbon, arciform density, and pedicle membrane, is closely apposed to the plasmalemma. Note the small dimple at the cell surface (arrowhead) opposite another synaptic vesicle. The enlarged cleft between the adjoining horizontal cell dendrites (*HD*) is bisected by a median plate and bridged by a regular array of crossbars (arrows). A layer of fluffy cytoplasmic material decorates the inner aspect of the membrane of the horizontal cell dendrites (*HD*) at the interface with all adjoining processes, but no such material is found beneath the membrane of the invaginating midget bipolar dendrite (*IMBD*). × 160,000.

FIGURE 4 *Macaca arctoides*. Specialized junction between neural processes in the neuropil underlying a cone pedicle; note the median plate and the crossbars in the enlarged intercellular cleft. A layer of fluffy material is seen beneath the plasmalemma. × 133,000.

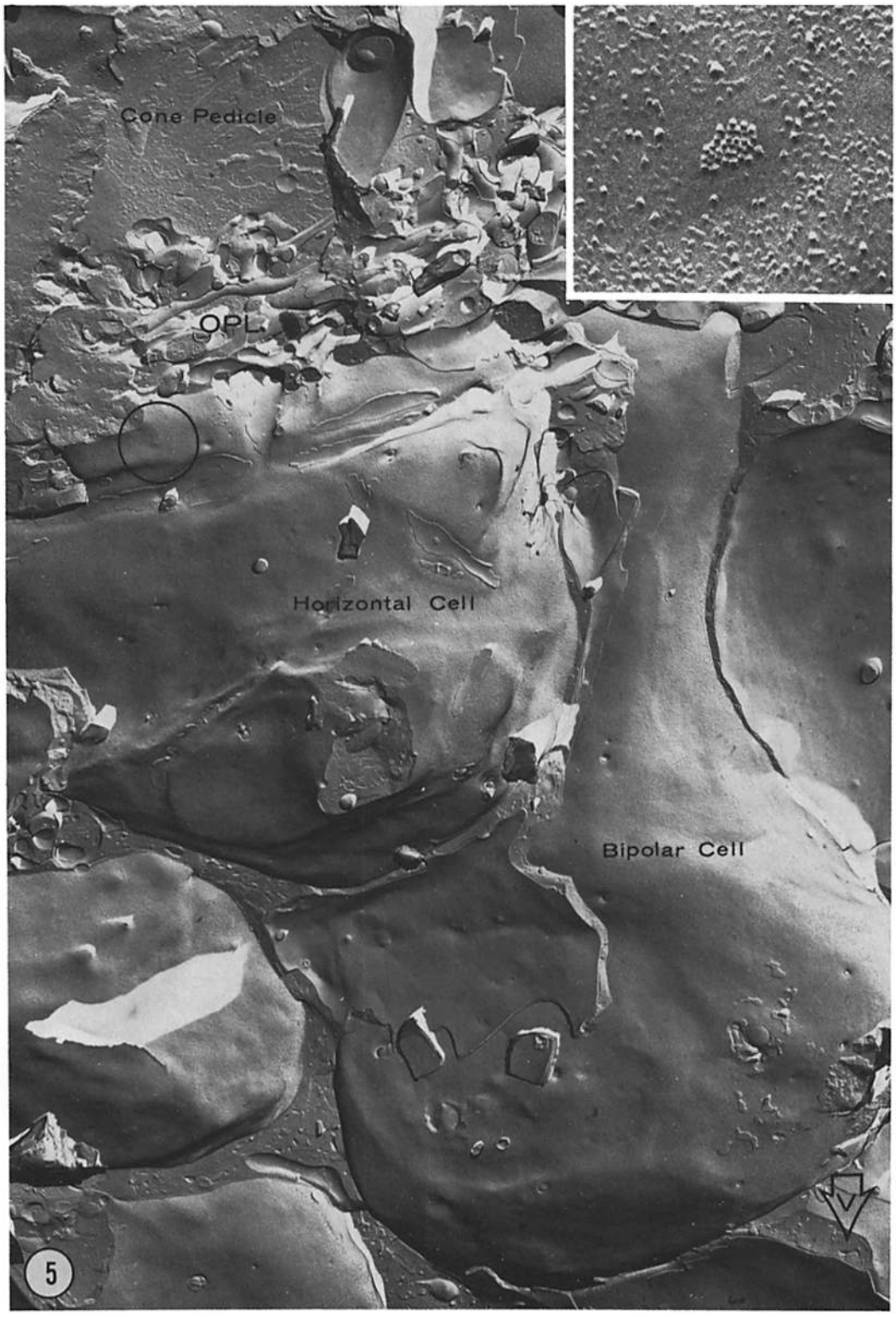

FIGURE 5 *Macaca arctoides*, freeze-fracture view of the outer plexiform (*OPL*) and part of the inner nuclear layers. Horizontal and bipolar cells are easily recognized on the basis of their shape and topography. A small gap junction is seen on the membrane A face of a horizontal cell (encircled area, enlarged in the inset). Note the halo of bare membrane matrix which surrounds the cluster of particles. × 11,000. Inset, × 115,000.

the B face of the membrane of the invaginating midget bipolar dendrite. Fig. 6 *a* is a representative image of this set of fractures and the diagrams in Figs. 6 *b* and 6 *c* illustrate the course of the fracture plane in two imaginary sections cut perpendicularly to the replica along lines 1 and 2. (*c*) The cleavage plane may intersect the plane of symmetry of the synapse along a line parallel to the apex of the synaptic ridge (Fig. 7). One slope of the ridge is then exposed throughout its length together with the A face or the B face of the membrane on the medial surface of one horizontal cell dendrite and either the A face or the B face of the membrane of the invaginating midget bipolar dendrite. The analysis of a number of such images confirms the time-honored views on the three dimensional configuration of this synapse: two sausage-like terminals of the horizontal cell dendrites lie on either side of a gently curving, 0.7–1-μm long synaptic ridge. With their concave medial aspect, the horizontal cell dendrites bound a fossa in which the tip of the invaginating midget bipolar dendrite is inserted.

The portion of the pedicle membrane which invests the synaptic ridge is highly specialized, and three morphologically and functionally distinct regions can be recognized: (*a*) at the apex of the ridge; (*b*) on its slopes; and (*c*) at the bottom of the valleys which flank the ridge on either side.

At the apex is an aggregate of particles which remain preferentially associated with the cytoplasmic portion of the membrane and leave a complementary set of pits on the B fracture face (Figs. 6 *a*, 7, 9, 11). The aggregate follows the apex of the ridge throughout its length and extends about 80 nm on either slope of the ridge; it is thus strikingly coextensive with the underlying arciform density. It consists of about 400 randomly dispersed particles, 9–11 nm in apparent diameter. They are polyhedral in shape and often contain a minute central dimple. The particles tend to be less numerous at the very summit of the ridge than on either side of it.

The appearance of the rest of the membrane that invests the slopes of the ridge varies in different pedicles. Most commonly, a row of tiny protuberances on the membrane B face parallels the apex of the ridge and is separated from it by a distance of 100 nm (Fig. 8). The protuberances have a diameter of 9–17 nm and are regularly spaced 45–80 nm apart. They vary in shape from a conical protrusion to a smooth bump, barely projecting above the surrounding membrane matrix. They are complemented on the membrane A face by a row of shallow pits. In other synaptic ridges a second, shorter row of B-face protuberances, and sometimes a third one are deployed laterally to the first one; in the last instance protuberances may be arranged in a planar hexagonal lattice with a unit cell side of 45–80 nm (Fig. 9). The distance of the protuberances both from each other and from the apex of the ridge is identical to the spacing of the vesicles aligned in rows on either side of the arciform density. Thus, there is no doubt that these localized features of the pedicle membrane fracture face correspond to sites of interaction between synaptic vesicles and plasmalemma. However, the resolution of our replicas is inadequate to determine whether the B-face protuberances belong to the population of the intramembrane particles or rather represent minute deformations of the plasma membrane.

In a small number of synaptic ridges, the sites of interaction between vesicles and plasmalemma, particularly those located next to the arciform density, are indicated by a pleiomorphic population of membrane specializations which on the B face include (Figs. 10, 15): (*a*) smooth hemispherical protrusions up to 25 nm in diameter; (*b*) "volcanos" with a 20 nm crater; (*c*) cylindrical studs 30 nm in diameter, with a slightly serrated edge; and (*d*) cylindrical protrusions 40 nm in diameter, bearing particles at their periphery. The complementary A-face specializations include: (*a*) shallow dimples; (*b*) particle rosettes 35 nm in diameter; and (*c*) cylindrical depressions 20–35 nm in diameter. This set of membrane specializations has been variously named synaptopores (1), presynaptic membrane modulations (51), vesicle attachment sites (37), and synaptic vesicle sites (17). They were recently shown to represent different stages of discharge of synaptic vesicles (17, 38). Finally, synaptic ridges are found which completely lack vesicle sites.

The membrane of the synaptic ridge contains a sparse population of particles lateral to the region of the vesicle sites (Fig. 12). These particles are either randomly dispersed or aggregated in small clusters. They tend to have a large diameter (10–15 nm), and are associated with both membrane fracture faces.

The bottom of the valleys which flank either side of the synaptic ridge is rarely exposed by the fracture process. In a few instances, however, rows of dimples are present on the membrane A face, with particles clumped at the bottom (Fig. 12);

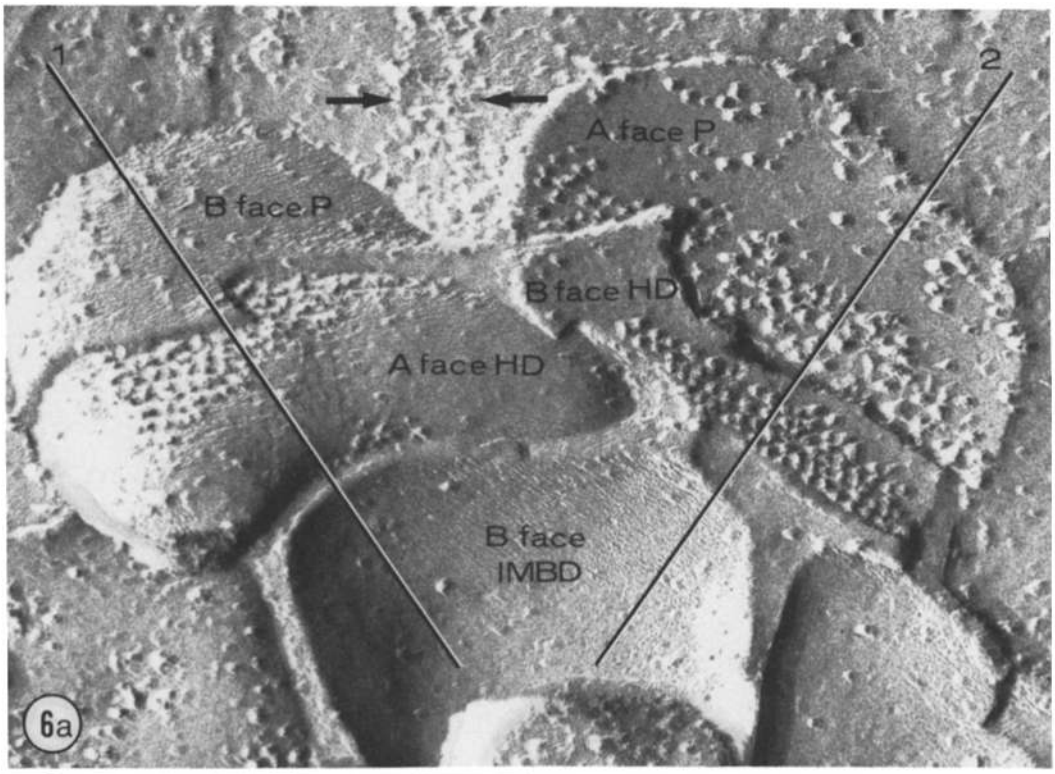
1
2
A face P
B face P
B face HD
A face HD
B face
IMBD
6a

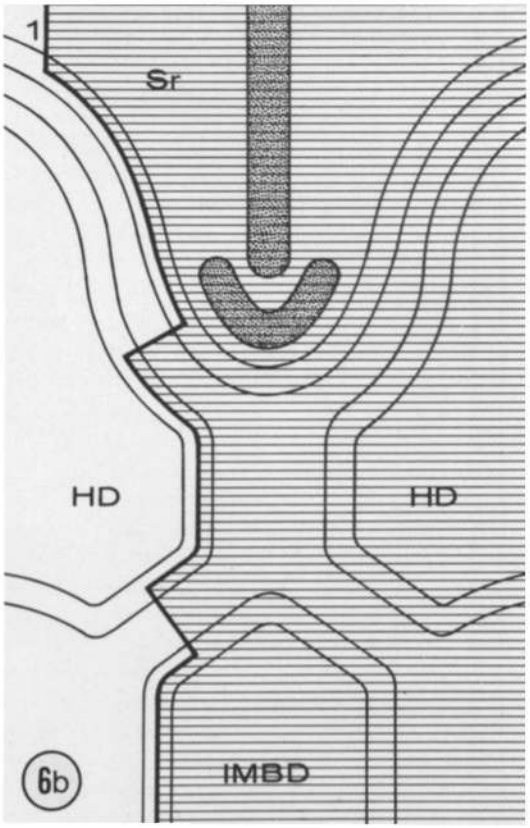
1
Sr
HD
HD
IMBD
6b

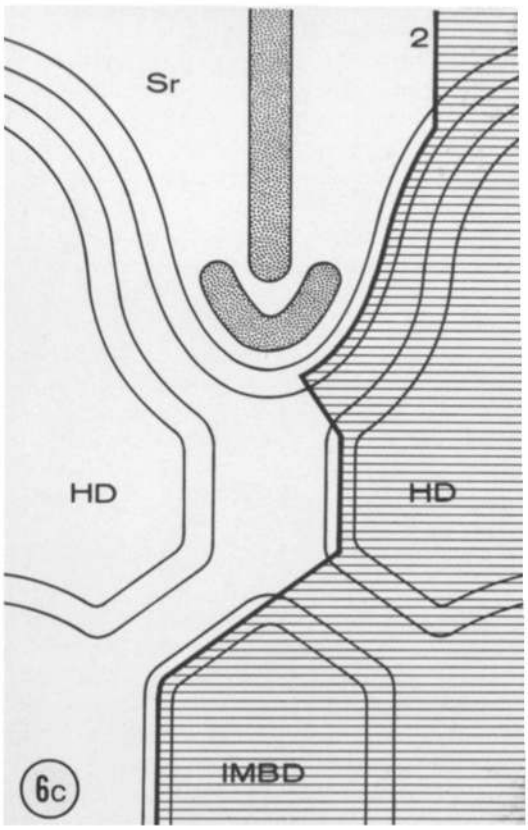
2
Sr
HD
HD
IMBD
6c

they are complemented by rows of volcanos on the membrane B face. Similar membrane features have been recently interpreted as intramembrane events which accompany the formation of coated vesicles from the plasmalemma (25).

The pedicle membrane which bounds the rest of the synaptic invagination is unremarkable, except for minute specializations that are present at the mouth of the invagination, where the pedicle membrane is molded upon the neck of the incoming dendrites. Here, short digitations of the pedicle fill in the intervals between the invaginating processes and often contact each other at rounded spots 0.1–0.2 μm in diameter. These cone-to-cone junctions (Fig. 14) resemble desmosomes of squamous epithelia with their population of randomly distributed, irregularly elongated particles which are associated with both fracture faces (28).

The membrane of each horizontal cell dendrite is specialized at the interface with (*a*) the synaptic ridge, (*b*) the adjoining horizontal cell dendrite, and (*c*) the tip of the invaginating midget bipolar dendrite. Elsewhere, it contains the usual complement of randomly distributed particles which are preferentially associated with the A face. Vesicle sites are consistently absent within the membrane of the horizontal cell dendrites.

Opposite the apex of the synaptic ridge is an elongated aggregate of particles which remain preferentially associated with the A face of the plasmalemma and leave a complementary set of pits on the B face (Figs. 8, 10, 11). Examination of a large number of replicas indicates that the elongated aggregate is coextensive with the apex of the synaptic ridge. Its width is about 100 nm which is narrower than the underlying layer of fluffy material on the inner aspect of the plasmalemma. Its geometrical projection on the synaptic ridge overlaps the apical A face particle aggregate of the pedicle membrane (Fig. 11). The particles are randomly distributed within the aggregate with an apparent diameter of 9–11 nm and a polyhedral shape. Frequently, they also contain a central dimple.

At the interface between the two horizontal cell dendrites, the adjoining membranes contain symmetrical arrays of particles that remain consistently associated with the membrane B face and leave a complementary set of pits on the membrane A face (Figs. 11–13). The two particle arrays are in perfect register with each other across the enlarged median cleft of the synaptic invagination. *En face* views of the medial aspect of the horizontal cell dendrites demonstrate that the B-face particle array is an elongated, gently curved band which is contiguous and parallel to the A-face particle aggregate previously described in the interior of the membrane of the horizontal cell dendrites (Figs. 11, 13). The array is 0.3–0.7 μm long and 60 nm wide; it consists of 60–150 particles, 13 nm in diameter, polyhedral in shape with a central dimple. The particles are aligned in parallel rows, directed perpendicularly to the apex of the synaptic ridge, and each row consists of 3–5 units. The interrow distance, measured from center to center of the particles, is highly consistent, averaging 17 nm; whereas the spacing along the rows varies from apparent fusion of neighboring particles to 20 nm. In many instances, however, the lattice of this specialization appears distorted or skewed, for the parallel rows extend in an oblique direction with respect to the apex of the ridge; this can be explained on the basis of an alteration of the shadow angle due to the curvature of the membrane specialization.

A third differentiation within the membrane of the horizontal cell dendrites, contiguous to the previous one, is found at the interface with the tip of the invaginating midget bipolar dendrite. It consists of a macular aggregate of particles which remain associated with the cytoplasmic portion of the membrane and leave a complementary set of

FIGURE 6 *a* *Macaca arctoides*, invaginating synapse of a cone pedicle. The fracture process has obliquely cut through the synaptic ridge, and exposed on either side of it the B face (*B face P*) and the A face (*A face P*) of the pedicle plasmalemma. Furthermore, it has exposed the A face of one horizontal cell dendrite (*A face HD*) and a small portion of the B face of the other horizontal cell dendrite (*B face HD*). Finally the B face of the invaginating midget bipolar dendrite (*B face IMBD*) is also exposed. Two imaginary sections cut perpendicularly to the replica along lines 1 and 2 are illustrated in Fig. 6 *b* and *c*. In the cytoplasm of the pedicle, the synaptic ribbon (arrows) appears as an array of irregular protrusions emerging from the cytoplasmic matrix. × 162,000. Fig. 6 *b* Diagram of an imaginary section cut perpendicularly to the replica of Fig. 6 *a* along line 1. The shaded area has been removed by the fracture process. *Sr*, synaptic ridge; *HD*, horizontal cell dendrite; *IMBD*, dendrite of an invaginating midget bipolar cell. Fig. 6 *c* Diagram of an imaginary section cut perpendicularly to the replica of Fig. 6 *a* along line 2. The shaded area has been removed by the fracture process. Symbols as in Fig. 6 *b*.

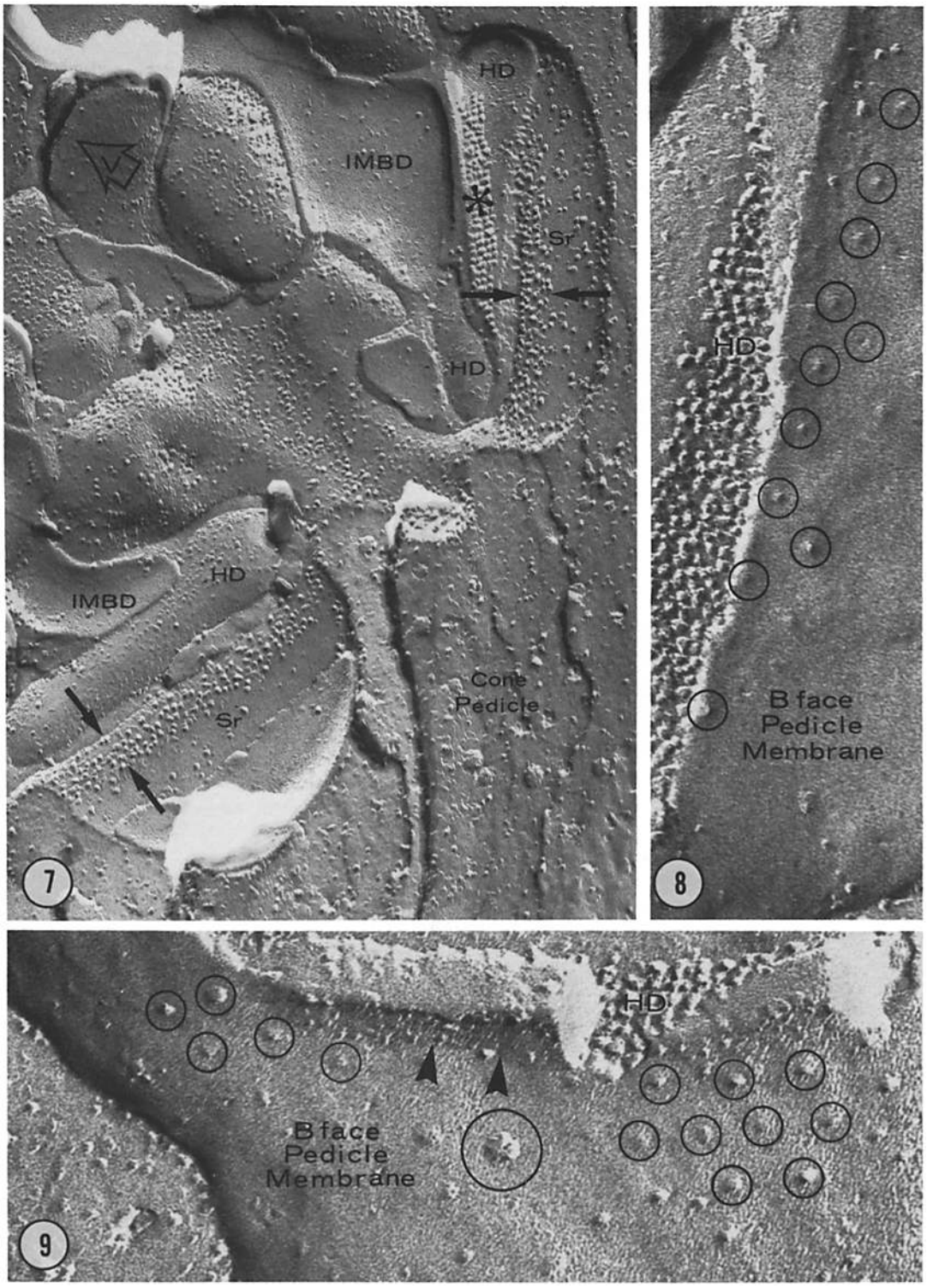
HD
IMBD
Sr
HD
IMBD
HD
Sr
Cone
Pedicle
7
HD
B face
Pedicle
Membrane
8
HD
B face
Pedicle
Membrane
9

pits on the membrane B face (Figs. 10, 11). These intramembrane components resemble those found at the interface between synaptic ridge and horizontal cell dendrites in their shape, size, and random distribution.

The interior of the plasmalemma of the invaginating midget bipolar dendrite is unspecialized (Fig. 12, 13). Randomly distributed particles uniformly stud the A fracture face, both outside and inside the synaptic invagination, whereas the B face is almost devoid of particles. At the tip of the dendrite, the contact region with the horizontal cell dendrites is characterized by particles less numerous than elsewhere (Fig. 13). Thus, in primates there is no freeze-fracture indication of the distal junctions described in the pedicles of thin-sectioned turtle retinas (27).

The vitreal surface of cone pedicles is gently undulating, with many shallow impressions each corresponding to a basal contact with a dendrite of a flat midget or diffuse cone bipolar (flat bipolar dendrites). Deeper fossae are also present, which represent the mouths of the synaptic invaginations and these are invariably occupied by cross-fractured dendrites of horizontal and bipolar cells. Particles on the A face of the pedicle membrane are more numerous at the impressions which mark the site of the basal contacts than over the intervening system of shallow ridges (Fig. 14). However, if A-face particle numbers at basal contacts are compared to those seen on the lateral surface of the pedicle, no significant difference is found. The B face of the membrane on the basal surface of pedicles has the usual sparse population of randomly distributed particles; vesicle sites are consistently lacking. Frequently, the fracture plane deviates from the interior of the pedicle membrane, crosses the intercellular cleft, and penetrates into the interior of the plasmalemma of the adjoining flat bipolar dendrites, thus exposing side by side their B face and the A face of the pedicle membrane. In these instances an aggregate of B-face particles is found at the tip of the flat bipolar dendrites, in register and coextensive with the impressions on the vitreal surface of the cone pedicle (Fig. 15). Each aggregate consists of 50–100 randomly distributed particles, about 12 nm in apparent diameter, polyhedral in shape, and often with a small central dimple. The cytoplasmic half of the membrane of the flat bipolar dendrites has numerous, randomly distributed particles, except at the contact region with the vitreal surface of the pedicles, where a small bare region is occasionally found.

In summary (Figs. 1 and 16), on the slopes of the synaptic ridge of pedicle invaginating synapses an aggregate of intramembrane A-face particles, a hexagonal array of synaptic vesicle sites, and rows of coated vesicle sites are sequentially arranged from apex to base. Across an enlarged intercellular cleft, the adjoining membrane of the horizontal cell dendrites contains an aggregate of A-face particles and bears a layer of dense material on its cytoplasmic surface. At the specialized junction between adjoining horizontal cell dendrites the intercellular cleft is considerably enlarged, bisected by a dense plate, and traversed by uniformly spaced crossbars. The adjoining membranes contain symmetrical arrays of B-face particles arranged in parallel rows and bear a layer of dense material on their cytoplasmic surface. At the specialized junction between horizontal cell and invaginating midget bipolar dendrites the intercellular cleft is slightly enlarged. The membrane of

FIGURE 7 *Macaca arctoides*. Two synaptic ridges (*Sr*) of a cone pedicle are exposed throughout their length. An aggregate of particles (arrows), which remain associated with the A face, is present at the apex of the ridges. The asterisk labels the B-face particle aggregate of a horizontal cell dendrite (*HD*). *IMBD*, invaginating midget bipolar dendrite. × 76,000.

FIGURE 8 *Macaca mulatta*, perifoveal pedicle. A row of tiny synaptic vesicle sites (circles) is deployed on the membrane B face along the slope of a synaptic ridge. The row is very close to the apical aggregate of A-face particles, for the fracture plane has penetrated the membrane of the adjoining horizontal cell dendrite (*HD*) and exposed its A-face specialization, which lies in register with the apical aggregate of the synaptic ridge. × 174,000.

FIGURE 9 *Macaca mulatta*, perifoveal pedicle. On the slope of a synaptic ridge, vesicle sites (circles) may occur in hexagonal array. The upper row is very close to a pitted region (arrowheads) of the membrane B face, which represents the complementation of the apical aggregate of A-face particles. The fracture process has also exposed part of the A-face particle aggregate of the adjoining horizontal cell dendrite (*HD*). × 182,000.

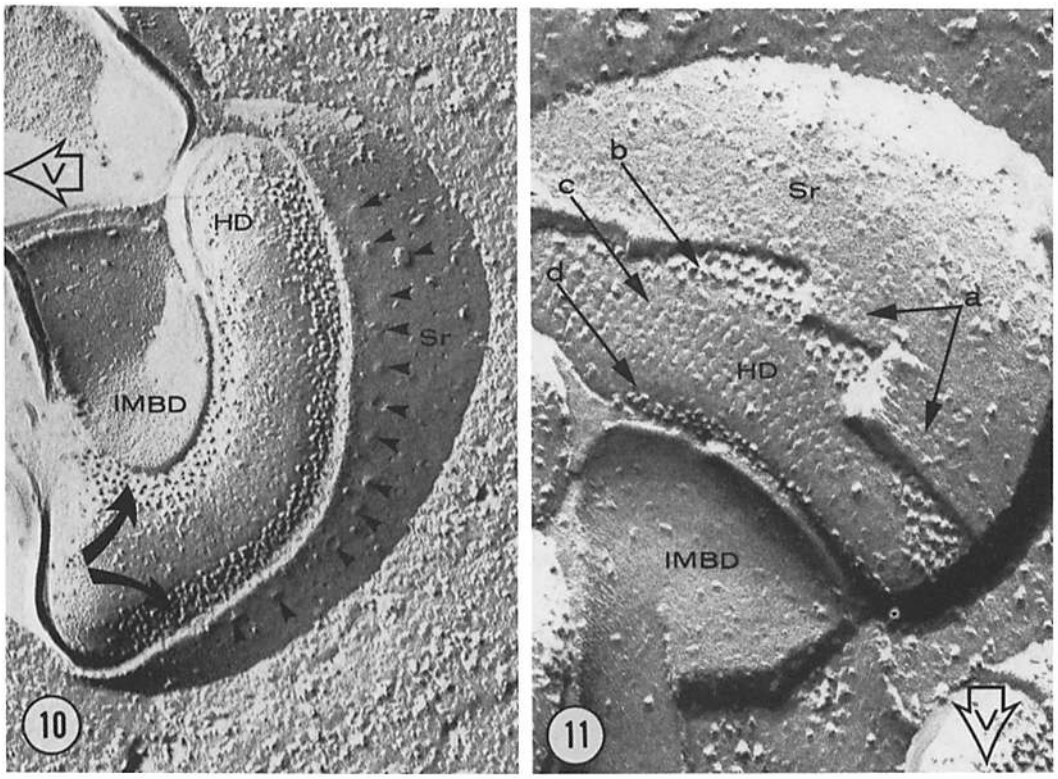

FIGURE 10 *Macaca mulatta*, cone pedicle. The course of the fracture plane is identical to that illustrated in Fig. 6 *b*. Large forms of vesicle sites (arrowheads) are aligned in a row on the B face of the membrane which invests the slope of a synaptic ridge (*Sr*). The plasmalemma on the medial aspect of the horizontal cell dendrite (*HD*) has two aggregates of A-face particles (arrows), one opposite the apex of the ridge, the other opposite the tip of the invaginating midget bipolar dendrite (*IMBD*). × 88,000.

FIGURE 11 *Macaca arctoides*, cone pedicle. This image also conforms to the diagram of Fig. 6 *b*. On the slope of the synaptic ridge (*Sr*) vesicle sites are not present; a pitted region (*a*) is seen near the apex of the ridge, where the fracture process has removed the A-face particle aggregate. On the medial aspect of the horizontal cell dendrite (*HD*) the membrane contains: (*b*) an aggregate of A-face particles, partially concealed by the pedicle membrane; (*c*) a pitted region where the horizontal cell dendrite adjoins its partner process across the median gap of the invaginating synapse (here B-face particles have been removed by the fracture process); and, (*d*), an aggregate of A-face particles, partially concealed by the membrane of the invaginating midget bipolar dendrite (*IMBD*). × 118,000.

FIGURE 12 *Macaca mulatta*, cone pedicle. The fracture plane has split two invaginating synapses according to the diagram in Fig. 6 *c*, and exposed an extensive region of the membrane A face of the synaptic ridge (*Sr*). Three contiguous domains are deployed within the plasmalemma that invests the slopes of the ridges. (*a*) The apical region with a particle aggregate (arrows). (*b*) The intermediate region, characterized by a sparse population of large particles, either dispersed or congregated in small clusters; this is the region where synaptic vesicles usually interact with the plasma membrane. (*c*) The basal region, typically occupied by dimples containing clumps of particles (arrowheads), which may represent sites of formation of coated vesicles. In both synapses the membrane of the horizontal cell dendrites (asterisks) contains a prominent array of B-face particles arranged as an elongated, gently curving band. The membrane B face of the invaginating midget bipolar dendrite (*IMBD*) is broadly exposed and this appears unspecialized. Note a small gap junction (circle) in the neuropil underlying the cone pedicle. × 58,000.


Sr
IMBD
Sr
IMBD
V
12

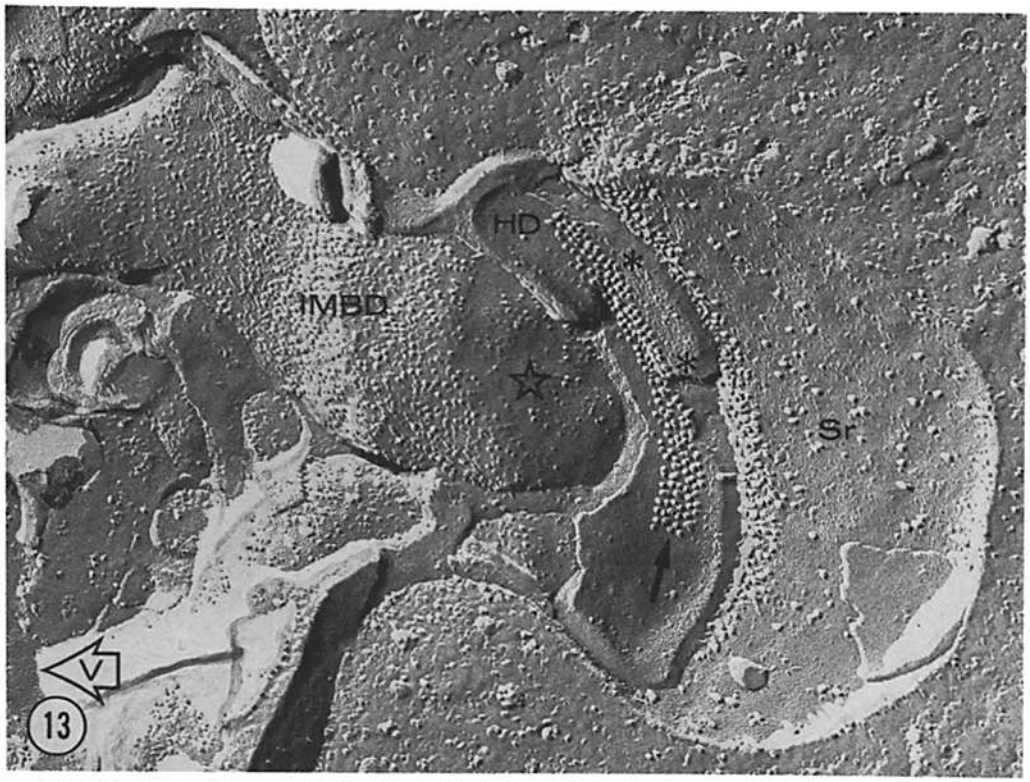
HD
IMBD
Sr
V
13


Cone Pedicle
14

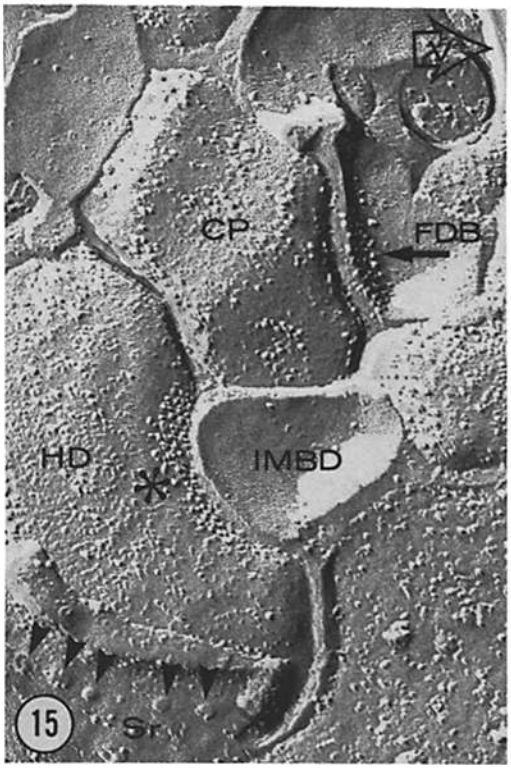
CP
FDB
HD
IMBD
15
Sr

the horizontal cell dendrites contains an aggregate of A-face particles and bears a layer of dense cytoplasmic material, whereas the adjoining plasmalemma of the invaginating midget bipolar dendrite is unspecialized. At the basal contacts, the intercellular cleft is enlarged and contains dense material; in the pedicle membrane, A-face particles are moderately clustered, whereas the adjoining membrane of the flat bipolar dendrites contains an aggregate of B-face particles. Furthermore, both adjoining membranes have an undercoat of dense cytoplasmic material. At the neck of the synaptic invagination, small desmosomes interconnect cone pedicle digitations that fill in the interstices between the incoming dendrites. Synaptic vesicle sites occur neither on the surface of the horizontal cell dendrites nor at the basal contacts.

ROD SPHERULES: Cross-fractured spherules (Fig. 17) contain a population of round synaptic vesicles, 45 nm in diameter with particles embedded in their limiting membrane. The noninvaginated portion of the spherule plasmalemma has rows of gap junctional subunits (43) and a rich complement of randomly distributed particles which are preferentially associated with the A fracture face. The particle concentration, however, tends to decrease in the proximity of the synaptic invagination. In most spherules, an additional, unusual specialization is present in the interior of the plasmalemma: linear aggregates of short strands, interspersed with particles, either irradiate from the mouth of the synaptic invagination or occur in parallel arrays on the lateral surface of the spherule (Fig. 18). The identity of the aggregates is less distinct as the distance from the invagination increases; eventually, they appear to merge with the surrounding population of randomly dispersed particles. These linear aggregates of strands and particles preferentially cleave with the A face, leaving short furrows and pits on the B face. They do not represent intramembrane components of an intercellular junction, because they are absent within the plasmalemma of the adjoining cell, usually a Müller cell process (Fig. 18, inset). Their counterpart in thin-sectioned retinas has not been identified.

In the invaginating synapse, the ridge displays membrane structure similar to that found in cone pedicles. The apical A-face cluster (Fig. 19) consists of about 500 particles. It is separated by an enlarged intercellular cleft from a symmetrical aggregate of A-face particles in the membrane of the adjoining axonal endings of the horizontal cells. The aggregate in the horizontal cell endings is 1 μm long, 50–120 nm wide, and is flanked by a membrane region almost devoid of particles (Fig.

FIGURE 13 *Macaca mulatta*, invaginating synapse of a cone pedicle. The fracture process has exposed the membrane A face of a synaptic ridge (*Sr*), the B face of the membrane on the medial aspect of a horizontal cell dendrite (*HD*), and the membrane A face of the invaginating midget bipolar dendrite (*IMBD*). The membrane B face of the horizontal cell dendrite is characterized by an array of particles (arrow) opposite the adjoining horizontal cell dendrite and a pitted area (asterisks) opposite the apex of the ridge; these pits complement the A-face particle aggregate which has been removed by the fracture process. The A face of the membrane of the invaginating midget bipolar dendrite (*IMBD*) is studded with randomly distributed particles both outside and inside the synaptic invagination. However, at the contact region with the horizontal cell dendrite (*HD*), the tip of the bipolar dendrite has particles somewhat less numerous than elsewhere (star). × 70,000.

FIGURE 14 *Macaca mulatta*. On the basal surface of a perifoveal cone pedicle shallow impressions are seen, each corresponding to a basal contact with a flat midget or diffuse cone bipolar cell; particles on the A face of the pedicle membrane are more numerous at the impressions (outlined areas) than over the intervening shallow ridges. The arrow indicates a small desmosome which connects interdigitating processes of the cone pedicle at the neck of a synaptic invagination. × 53,500.

FIGURE 15 *Macaca mulatta*, cone pedicle. The fracture process has exposed an invaginating synapse according to the diagram of Fig. 6 *a*. A row of large synaptic vesicle sites (arrowheads) is present on the membrane B face of the synaptic ridge (*Sr*). The A-face particle aggregate at the interface between a horizontal cell dendrite (*HD*) and the invaginating midget bipolar dendrite (*IMBD*) is indicated by an asterisk. This micrograph also illustrates a basal contact between the vitreal surface of the cone pedicle (*CP*) and an adjoining dendrite of a flat midget or diffuse cone bipolar cell (*FBD*). A cluster of particles (arrow) on the membrane B face of the dendrite lies in register with a shallow impression of the pedicle basal surface. × 76,000.

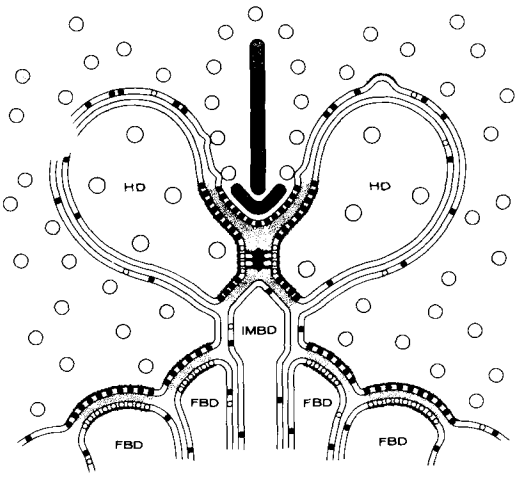

FIGURE 16 Diagram of the intramembrane specializations of cone pedicle synapses in the primate retina. Particles which remain preferentially associated with the cytoplasmic portion of the membrane (A face) are represented as solid circles; particles which remain preferentially associated with the external portion of the membrane (B face) are represented as open circles. *HD*, horizontal cell dendrite; *IMBD*, invaginating midget bipolar dendrite; *FBD*, dendrites of flat midget and diffuse cone bipolar cells.

20). The rest of the membrane of the horizontal cell endings has the usual population of randomly distributed particles preferentially associated with the membrane A face. Thus, in contrast to horizontal cell dendrites in pedicle synapses, the axonal endings of the horizontal cells in spherules contain neither a B-face particle aggregate at the interface with the adjoining horizontal cell ending, nor an A-face particle aggregate at the interface with the bipolar dendrites. The dendrites of the rod bipolar cells (Fig. 17) lack particle aggregates on their membrane B face, and they have randomly distributed particles on their membrane A face. The particles, however, decrease in number at the contact region with the axonal endings of the horizontal cells. In a few instances, a small gap junction connects processes of unknown origin within the synaptic invagination (Fig. 21).

In summary (Fig. 22), the plasmalemma that invests the synaptic ridge of rod spherules has an aggregate of A-face particles, an array of synaptic vesicle sites, and rows of coated vesicle sites arranged in order from apex to base. The adjoining membrane of the axonal endings of the horizontal cells contains an aggregate of A-face particles and bears a layer of dense material on its cytoplasmic surface. The remainder of the membrane of the axonal endings of the horizontal cells, and the plasmalemma of the rod bipolar dendrites are unspecialized.

INNER ZONE OF THE OUTER PLEXIFORM LAYER: Throughout the neuropil underlying the cone pedicles, prominent arrays of particles are present on the membrane B face of numerous cell processes (Fig. 23). They appear as square or rounded patches, about 250 nm in diameter, that consist of 150–200 particles arranged in parallel rows. The particles are 12 nm in diameter, polyhedral in shape, and often contain a small central dimple. Their interrow distance is 17 nm, whereas their spacing within the rows varies from apparent fusion of neighboring particles up to 20 nm. A complementary lattice of pits is found on the A face of the adjoining membrane when the fracture process exposes part of a B-face particle aggregate of one process and crosses the intercellular space into the interior of the plasmalemma of the neighboring process (Fig. 24). These slightly cross-fractured images also demonstrate that in the region of the particle array the intercellular cleft is enlarged and bridged in places by tenuous cross-strands. Thus, the prominent B-face particle arrays scattered throughout the neuropil beneath the cone pedicles belong to a symmetrical intercellular junction which represents the freeze-fracture counterpart of the desmosome-like specializations seen in thin-sectioned specimens. Furthermore, this junction is identical to the specialization which occurs at the interface between adjoining horizontal cell dendrites in the invaginating synapses of cone pedicles. Additional evidence that the interacting processes belong to the horizontal cells lies in the fact that arrays of B-face particles are often present on the scleral aspect of horizontal cell bodies, identified on the basis of their shape and location in the inner nuclear layer (Fig. 25). In a few instances the process containing an array of B-face particles was observed to terminate into a synaptic invagination of a cone pedicle as one of the deeply inserted lateral dendrites.

In the neuropil underlying the rod spherules, the fracture process frequently exposes bundles of processes which course in a vertical direction toward the synaptic invagination of spherules, and one of them frequently has longitudinal rows or small clusters of particles on its membrane B face (Fig. 25, inset). In a few instances, the process was continuous with a deeply inserted, lateral element of a synaptic invagination and could therefore be

FIGURE 17 *Macaca mulatta*. cross-fracture image of a rod spherule. A synaptic ridge (*Sr*) is identified by its apical aggregate of A-face particles; another ridge by the presence of the ribbon (arrowheads). The axonal endings of the horizontal cells (*HA*) are identified on the basis of their lateral position with respect to a synaptic ridge. Other invaginating processes (*RBD*) are likely to represent rod bipolar dendrites. × 52,000.

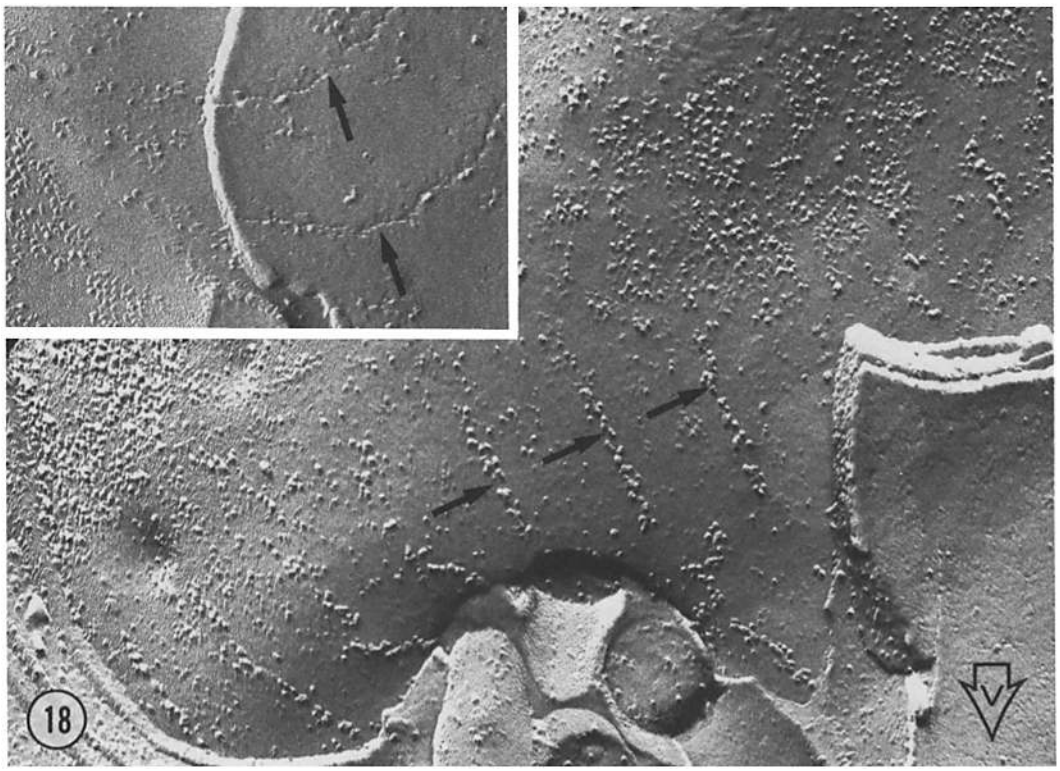

FIGURE 18 *Macaca mulatta*. The noninvaginated portion of the spherule membrane contains particles and short strands arranged in linear aggregates (arrows), which irradiate from the mouth of the synaptic invagination. They preferentially fracture with the cytoplasmic portion of the membrane and leave a complementary set of pits and furrows on the membrane B face (inset, arrows). These aggregates do not represent intramembrane components of an intercellular junction, for they are absent in the interior of the plasmalemma of the adjoining cell (inset). Note that particles are less numerous in the intervals between the aggregates. × 81,000. Inset, × 120,000.

identified as an ending of a horizontal cell axon. However, it is difficult to determine whether a symmetrical specialization also exists within the membrane of a neighboring process. This finding suggests that a specialized junction characterized by an array of intramembrane B-face particles may also occur between the two axonal endings of the horizontal cells which penetrate the synaptic invagination of each rod spherule.

Gap junctions are quite numerous throughout

FIGURE 19 *Macaca mulatta*, *en face* view of the apex of a synaptic ridge (*Sr*) in a rod spherule, with its aggregate of A-face particles. Note that particles are less in number at the very summit of the ridge. × 106,000.

FIGURE 20 *Macaca arctoides*. In the cross-fractured cytoplasm of a rod spherule, a synaptic ridge is identified by the presence of a synaptic ribbon (arrowheads). The ridge is flanked on either side by the axonal endings of the horizontal cells (*HA*), and one of these contains a prominent aggregate of A-face particles (arrows) opposite the apex of the synaptic ridge. Note the scarcity of particles in the immediate vicinity of the aggregate. × 62,000.

FIGURE 21 *Macaca mulatta*, rod spherule. Small gap junction (arrow) between two unidentified processes within the synaptic invagination. × 65,000.

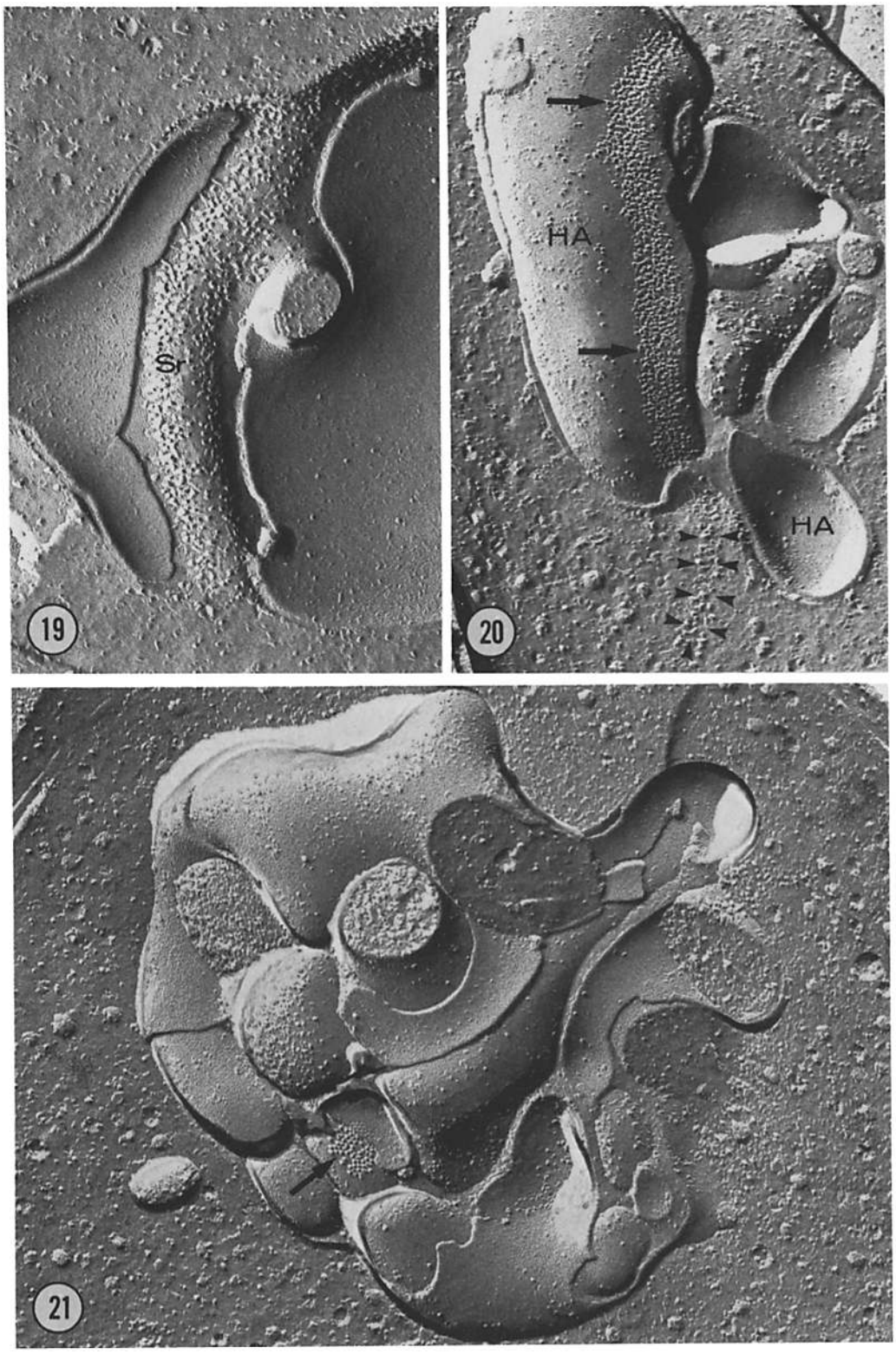
Sr
19
HA
HA
20
21

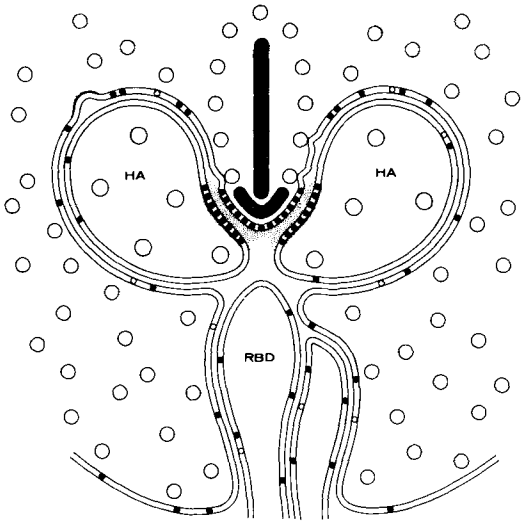

FIGURE 22 Diagram of the intramembrane specializations of the invaginating synapse of primate rod spherules. Solid circles, A-face particles; open circles, B-face particles; *HA*, axonal ending of a horizontal cell; *RBD*, rod bipolar dendrite.

the outer plexiform layer (Figs. 5, 12, 23); their small size explains why they have not been identified in previous studies on thin-sectioned primate retinas. In most cases the junctions are present as rounded or linear aggregates of 15–100 particles sitting on smooth bulges of the membrane A face or as small arrays of pits on the B face of neural processes extending through the layer. The junctional particles are 9–10 nm in diameter and appear clustered without obvious hexagonal packing. Less frequently, the full complement of features which characterize gap junctions is present, i.e. the aggregate of A-face particles lies opposite an array of pits on the B face of the adjoining membrane at a narrowing of the intercellular cleft. In some places, the identity of one of the partner cells can be unequivocally identified. Gap junctions are definitely established by: (*a*) invaginating midget bipolar dendrites in their course toward the synaptic invagination (they were identified on the basis of the median position assumed by their tip in the synaptic invagination); (*b*) flat bipolar dendrites, making basal contacts with the vitreal surface of pedicles; (*c*) horizontal cell dendrites in their course toward the synaptic invaginations of both pedicles and spherules (they were identified on the basis of the lateral location of their extremity with respect to a synaptic ridge); and (*d*) horizontal cell bodies (identified on the basis of their shape and location in the inner nuclear layer). However, it has never been possible positively to identify the origin of both adjoining processes. Finally, clusters of gap junctional particles commonly occur in close association with the arrays of B-face particles typical of the membrane of horizontal cell processes. Thus, the presence of minute gap junctions between horizontal cells is substantiated by adequate circumstantial evidence. Although the precise identity of the partner cell in the junctions established by cone bipolar dendrites is not known, it appears that a gap junctional system interconnects the bipolar dendrites which synapse with each cone pedicle.

Rabbit Retina. Freeze-Fractured Specimens

In cone pedicles the membrane of the synaptic ridge has a structure similar to that present in the monkey retina. The deeply inserted elements of the synaptic invagination which belong to horizontal cells (49), contain both an A-face particle aggregate opposite the apex of the synaptic ridge and a B-face particle array at the interface with the adjoining horizontal cell process (Fig. 26). The A-face particle aggregate has the shape of a plaque

FIGURE 23 *Macaca arctoides*. Throughout the neuropil beneath cone pedicles prominent arrays of particles (arrows) are present on the B face of the plasmalemma of numerous neural processes. They resemble the intramembrane specialization which occurs at the interface between adjoining horizontal cell dendrites in pedicle invaginating synapses (asterisk), and differ from gap junctions (circle), whose intramembrane particles remain associated with fracture face A. *Sr*, synaptic ridge. × 48,000.

FIGURE 24 *Macaca mulatta*, neuropil of the outer plexiform layer beneath a cone pedicle. The B-face particle array (*B*) of a cell process lies in register with an array of pits on the membrane A face of a neighboring process (*A*); thus, B-face particle arrays are contained within the membrane of both adjoining processes and represent the freeze-fracture counterpart of a symmetrical intercellular junction. Inset, the particles are arranged in parallel, equidistant rows. However, within each row the particle spacing is variable, and in some places the particles are fused. × 167,000. Inset, × 285,000.

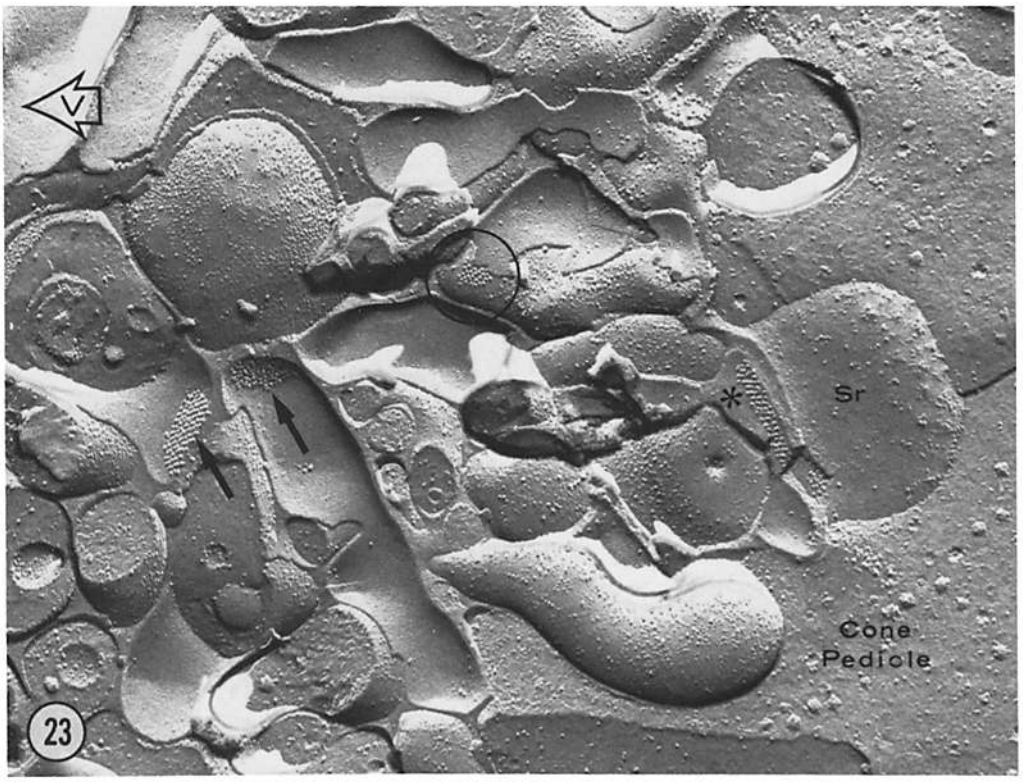
V
Sr
Cone
Pedicle
23

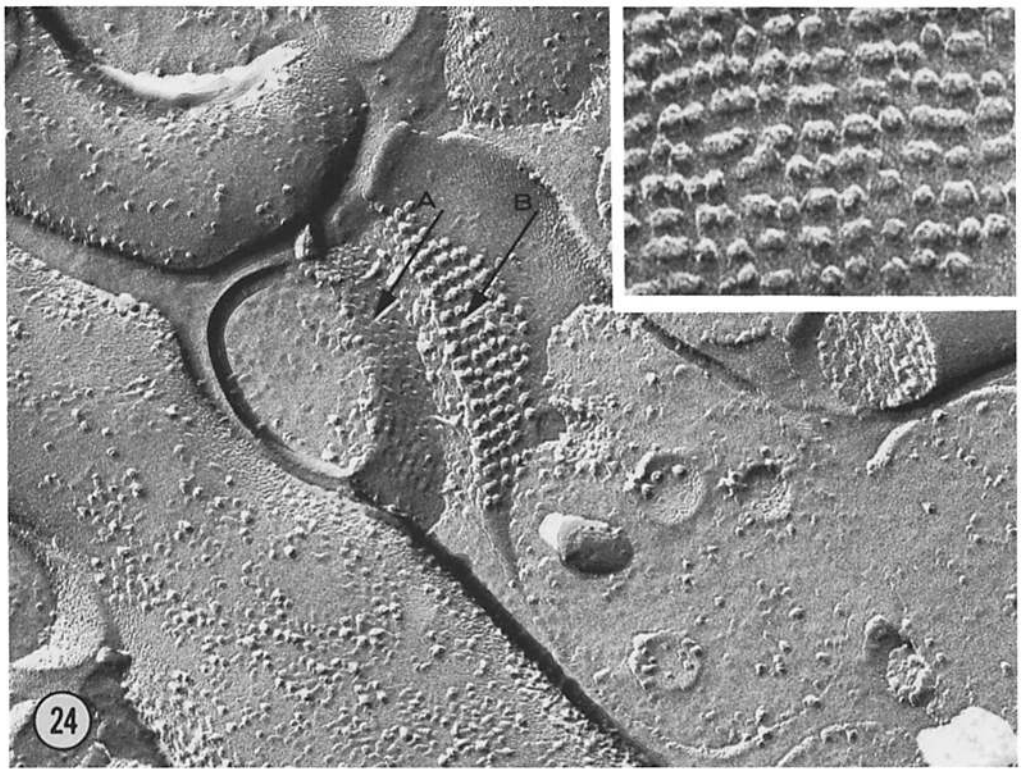
A
B
24

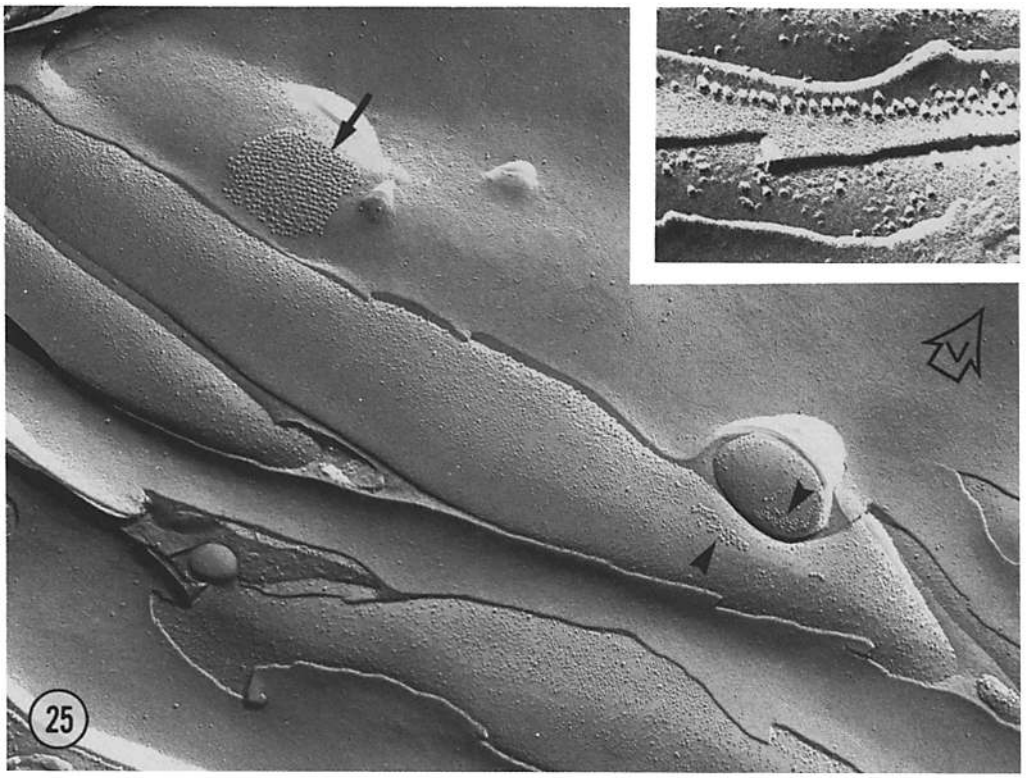
V
25

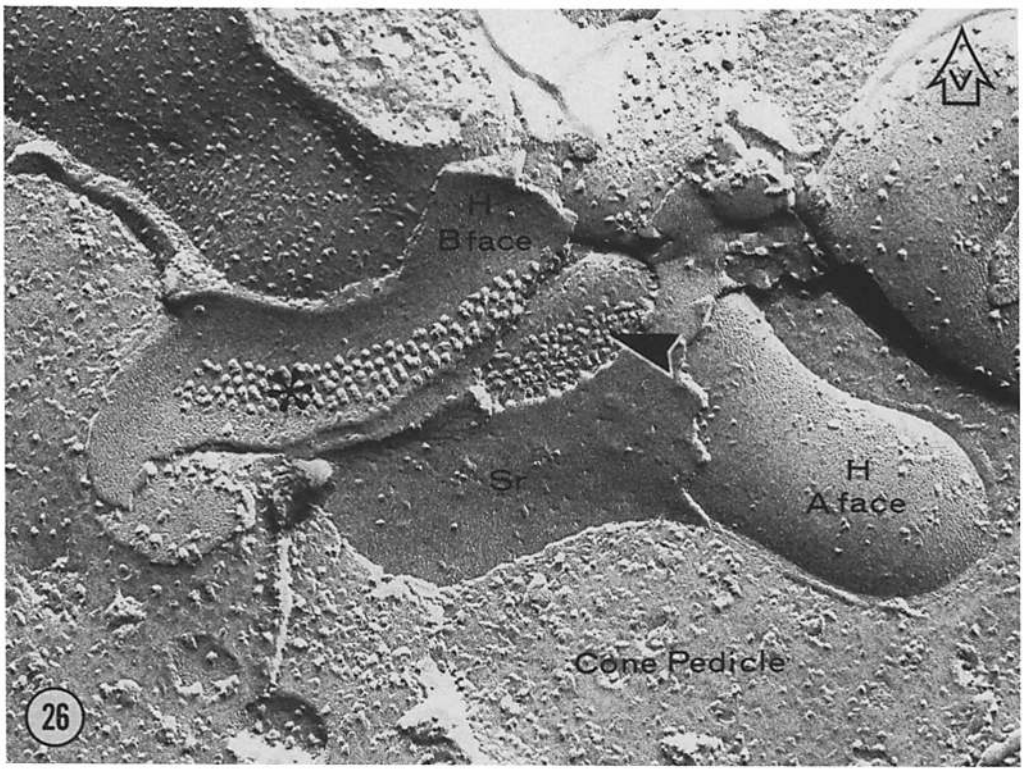
V
H
B face
Sr
H
A face
Cone Pedicle
26

lying contiguous to or even inserted into the B-face particle array (Fig. 27). At the basal contacts, the dendrites of the bipolar cells have an aggregate of particles on their B fracture face. To date, we have been unable to identify the dendrites of the invaginating cone bipolars.

The freeze-fracture organization of rabbit rod spherules does not differ significantly from that of monkeys. Linear arrays of intramembrane B-face particles are commonly found along the length of processes which ascend toward spherule invaginations.

In the neuropil underlying cone pedicles the B-face particle arrays which are typically found in the monkey are rarely observed. Aggregates of large particles are commonly present on the membrane A face of horizontal cell processes (Fig. 28). These aggregates probably represent the freeze-fracture counterpart of gap junctions seen in thin-sectioned specimens. However, their morphology is most unusual, because the particles are loosely arranged and thus their complementation on the B fracture face is rarely observed.

DISCUSSION

The freeze-fracture analysis of the neural connections in the outer plexiform layer of the retina demonstrates a remarkable diversity in the internal organization of the synaptic membranes. Specialized contacts between different types of neurons are characterized by highly specific arrangements of synaptic vesicle sites and intramembrane particles. Furthermore, particle aggregates in retinal synapses have a highly consistent location, shape, size, and affinity for the outer or inner portion of the membrane. There is evidence that synaptic vesicle sites are membrane differentiations associated with the interaction of synaptic vesicles with the plasmalemma (17, 38), but nothing is known about the functional significance and chemical identity of the particles contained in the interior of the synaptic membranes. However, recent studies have shown that numbers, arrangement, and fracture properties of the particles are different in excitatory and inhibitory synapses of the central nervous system (25, 26) and in peripheral cholinergic synapses (11, 13, 17, 41). Furthermore, observations on isolated cell membranes of *Torpedo* electric tissue seem to indicate that acetylcholine receptors are proteins largely buried in the plasma membrane and they may correspond to the intramembrane particles revealed by freeze-fracturing (8, 34). These observations, and our finding that precise particle arrangements define specific neuronal interfaces, clearly indicate that the internal structure of the synaptic membrane, as exposed by freeze-fracturing, is intimately correlated with synaptic function. Intramembrane particles may perhaps contribute to mechanical adhesion between the synapsing neurons, but they are also likely to represent ion channels, carry receptor sites for transmitter substances and regulatory mechanisms of membrane permeability.

In the primate retina, a material of choice for morphological studies of the outer plexiform layer, nothing is known about the interactions between photoreceptor, bipolar, and horizontal cells. Thus, any attempt to interpret the functional significance of the intramembrane specializations at the neural contacts of the outer plexiform layer has to be based on the assumption that the physiology of the distal neurons in the primate retina is basically the same as in nonmammalian species.

Synaptic Ridge of Photoreceptor Endings

Freeze-fracturing strongly supports the accepted view that the synaptic ridge represents a presynaptic zone at the surface of both pedicles and spherules, for its slopes display synaptic vesicle sites. However, in the same specimen vesicle sites

FIGURE 25 *Macaca mulatta*. An array of intramembrane B-face particles (arrow) is present on the scleral aspect of the body of a horizontal cell. The arrowheads indicate small clusters of gap junctional particles on the membrane A face of two unidentified cell processes of the outer plexiform layer. Inset, one of the processes which extend in a small bundle toward the synaptic invagination of a rod spherule, has a row of B-face particles in its plasmalemma. × 46,500. Inset, × 100,000.

FIGURE 26 Rabbit, invaginating synapse of a cone pedicle. The fracture process has exposed both fracture faces of the deeply inserted horizontal cell processes (*H*) which flank the synaptic ridge (*Sr*) on either side. One horizontal cell process has an intramembrane A-face particle aggregate (arrowhead) opposite the apex of the synaptic ridge. The other horizontal cell process has an array of B-face particles (asterisk) in register with the median gap of the invaginating synapse. × 128,000.

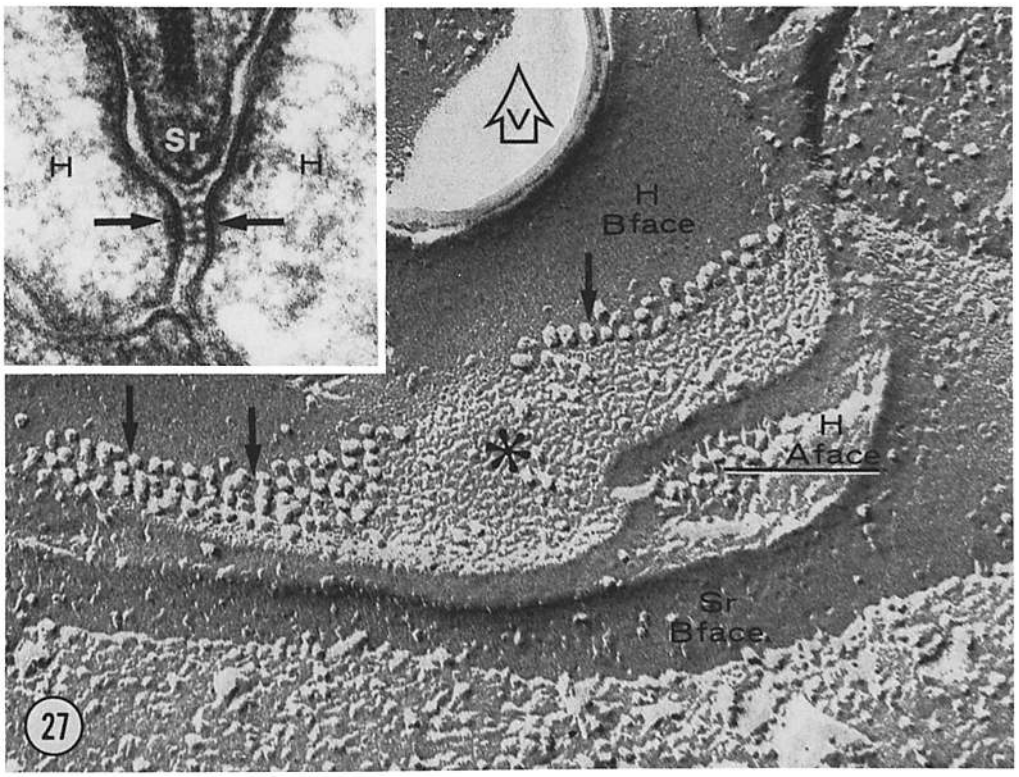
H
Sr
H
V
H
Bface
H
Aface
Sr
Bface
27

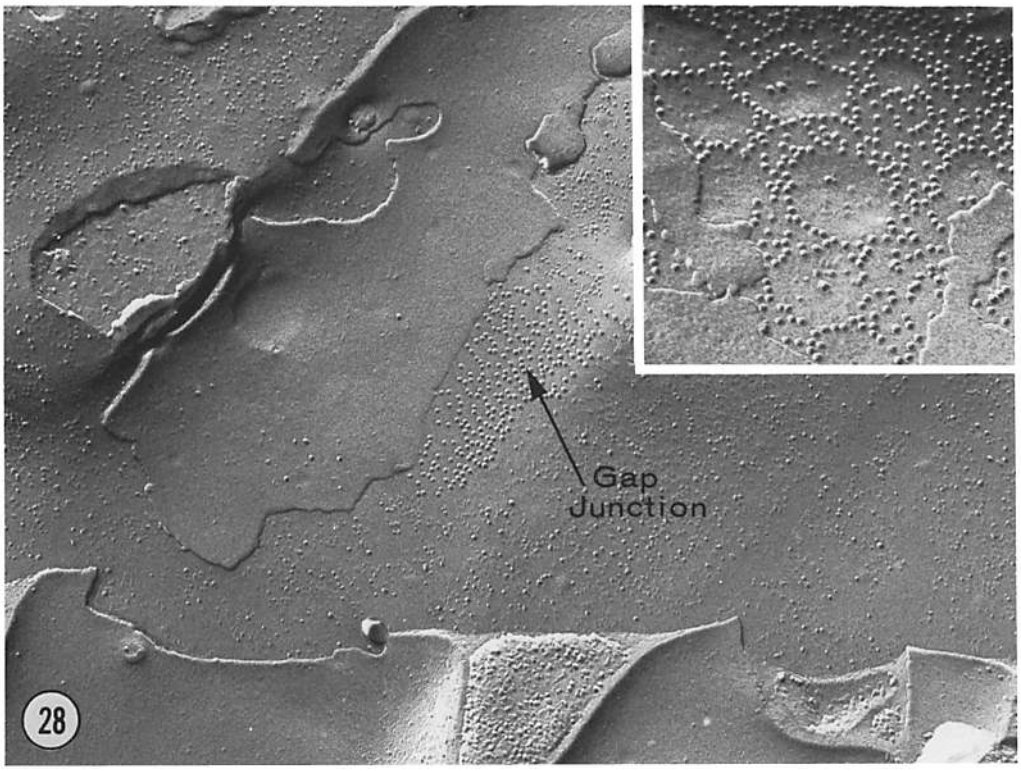
Gap
Junction
28

occur with varying frequencies in different photoreceptor endings and may be totally absent from a number of synaptic ridges. This confirms previous findings that vesicle sites represent transient differentiations of the presynaptic membrane (17, 38). Whether the numerical fluctuation of vesicle sites in different endings reflects the local result of light stimulation and antagonistic feedback of horizontal cells onto the photoreceptors was not investigated in the present study, in which no precaution was taken to standardize retinal illumination before or during fixation.

When the number of vesicle sites on the slope of a ridge is large enough, it becomes obvious that they are distributed in parallel rows and they may generate a planar hexagonal lattice. Their distance, both from each other and from the apex of the synaptic ridge, is identical to the spacing of the underlying synaptic vesicles; this is in agreement with previous observations that vesicle site distribution matches the arrangement of the synaptic vesicles interacting with the presynaptic membrane (17, 37). Since the distance between the vesicle sites on the slopes of the ridge is on the average larger than the diameter of the synaptic vesicles contained in the cytoplasm of the photoreceptor ending, the hexagonal deployment of vesicle sites is not dictated by close packing of the underlying synaptic vesicles. Clearly, synaptic vesicles do not interact randomly with the plasma membrane, and their mobility is restricted by extrinsic factors; either an orderly system of connections to the ribbon or a hexagonal deployment of binding sites on the inner aspect of the plasmalemma. We favor the former interpretation, since tenuous arms appear to connect the vesicles to the ribbon (15), and no permanent specialization occurs either within or on the inner aspect of the cell membrane. Also in central nervous system synapses vesicle sites may occur in hexagonal arrangement; the hexagons are not centered and each vesicle site seems to correspond to an opening of the centered hexagonal lattice of dense projections, which decorates the inner aspect of the presynaptic membrane (37). However, a major difference exists between the photoreceptor terminals and the presynaptic endings in central nervous system synapses, for the hexagons formed by the synaptic vesicle sites on the slopes of the ridge are centered, and there is no dense material on the inner aspect of the plasmalemma.

The regular distribution of the vesicle sites has enabled us to distinguish, in the spectrum of intramembrane features which mark the spot of interaction between synaptic vesicles and plasmalemma, a morphological configuration that escaped the attention of the previous investigators, who have analyzed synapses with the freeze-fracturing technique. Vesicle sites may appear as tiny protuberances on the B fracture face in the dimensional range of usual intramembrane particles, although smoother and perhaps shallower. It is not clear whether these protuberances represent intramembrane inclusions or minute inpocketings of the membrane as though an extremely localized traction is exerted on the plasmalemma. On theoretical grounds, a choice between these alternatives is crucial, for the presence of a membrane particle at the site of interaction between synaptic vesicle and plasmalemma supports the suggestion that a differentiation of the cell membrane binds synaptic vesicles and triggers their exocytosis (10). Particle rosettes in the plasmalemma of *Tetrahymena* seem to play such a role in mucocyst discharge (45). The lack of vesicle sites on many ridges does not represent a cogent objection to the hypothesis that these B-face protuberances represent vesicle binding sites, for the intramembrane

FIGURE 27 Rabbit, invaginating synapse of a cone pedicle. The fracture process has exposed the B face of the membrane at the apex of a synaptic ridge (*Sr B face*), and the membrane B face on the medial aspect of a horizontal cell process (*HB face*). A small portion of the membrane A face of the underlying horizontal cell process is also seen (*HA face*). The cluster of B-face particles (arrows) corresponds to the horizontal-to-horizontal cell junction illustrated in the inset (arrows). Also present in the B-face specialization is a pitted area (asterisk), which represents the complementation of the aggregate of A-face particles removed by the fracture process. × 170,000. Inset, × 126,000.

FIGURE 28 Rabbit, inner zone of the outer plexiform layer. An aggregate of large A-face particles is present on the scleral aspect of the body of a horizontal cell. Although the particles are somewhat loosely arranged, they probably belong to an unusual type of gap junction. In places, the particle aggregate resembles a lace (inset), as it encloses broad regions of smooth membrane matrix. × 60,000. Inset, × 99,000.

specializations which dictate the site of vesicle exocytosis need not be permanent or fixed in position. Vesicles may be bound to the ribbon and upon calcium entry into the ending may select the nearest binding site in a population of particles which move about randomly in the fluid domain of the plasmalemma. Alternatively, the B-face protuberances may represent a localized deformation of the plasma membrane upon vesicle attachment or vesicle retrieval, preparatory to or after exocytosis. This would imply that vesicle binding sites on the inner aspect of the plasmalemma do not penetrate the lipid domain of the membrane. The high frequency of the small forms of vesicle sites relative to the larger ones suggests that this phase has a longer life span or is more easily stabilized by the fixative fluid.

Large vesicle sites—hemispherical or "closed" (51), cylindrical, and volcano-like or "open" (51)—may well correspond to the critical stages of vesicle discharge. However, their minute size is an obstacle to the unequivocal identification of the complementary features on the A and B membrane faces, and therefore prevents a precise reconstruction of the membrane phenomena which accompany transmitter release.

The constellation of morphological specializations which characterize the synaptic ridge bears a striking resemblance to each of the structural units which are deployed many times along the length of the axonal ending in the neuromuscular junction (3, 9, 13, 16, 17). The ribbon and arciform density have their counterpart in the transverse bands of dense material which periodically underlie the axonal membrane, the apical aggregate of particles corresponds to the particle rows which flank the transverse bands, and, finally, in both cases synaptic vesicle sites and coated vesicle sites sequentially occupy contiguous domains of the plasmalemma on either side of the cytoplasmic differentiation.

The spatial segregation of the membrane specializations on the synaptic ridge is best explained by the hypothesis of synaptic vesicle membrane recycling, recently proposed for the frog neuromuscular junction (17). At the apex of the ridge the plasmalemma may be relatively stable, possibly because of its connections to the underlying arciform density. On either side of it, synaptic vesicle membrane may be added to the plasmalemma upon transmitter release, as evidenced by the presence of vesicle sites in freeze-fractured specimens and in thin sections by the undulating profile of the plasma membrane. More laterally, constituents of the synaptic vesicle membrane, possibly the particles swarming from the rows of vesicle sites, may migrate down along the slopes of the ridge to be retrieved by coated vesicles at the bottom of the valleys which flank the ridge on either side.

In this complex synapse, the arciform density may not only anchor the ribbon to the plasma membrane as previously suggested (15), but it may also function as a cytoskeleton for the ridge, which lacks microtubules. Furthermore, it may trap intramembrane components essential for the functioning of the synapse, and thus prevent their migration along the slopes of the ridge. The ribbon, in turn, may capture synaptic vesicles milling about in the ending and position them against the plasmalemma of the slopes of the ridge (7, 15). A similar function has been postulated for the dense material which decorates the inner aspect of the presynaptic membrane in the synaptic contacts of the superior cervical ganglion (36).

Dendrites and Axonal Endings of Horizontal Cells

Freeze-fracturing demonstrates a complex membrane structure for the horizontal cell processes which penetrate the invaginating synapses. In pedicles, each horizontal cell dendrite has an A-face particle aggregate opposite the apex of the synaptic ridge, an array of B-face particles opposite the adjoining horizontal cell dendrite, and an A-face particle aggregate opposite the tip of the invaginating midget bipolar dendrite. In spherules, the membrane of the axonal endings of horizontal cells only has an A-face particle aggregate at the interface with the synaptic ridge. Physiological studies in nonmammalian retinas suggest that a photoreceptor-to-horizontal cell synapse generates the hyperpolarizing response of luminosity horizontal cells to light stimulation of the photoreceptors (2); furthermore, in the turtle retina, luminosity horizontal cells depolarize cones, seemingly through a recurrent horizontal-to-photoreceptor cell synapse (2, 14, 35). In primates, a bidirectional interaction between photoreceptor and horizontal cells has been inferred from the presence of synaptic vesicles in both horizontal cell dendrites and axonal endings, and from the pattern of neural interconnections in the outer plexiform layer (12, 50). However, no freeze-fracture evidence is available to document a presynaptic function of the horizontal cells, for no synaptic vesicle sites occur at the surface of their processes in our conditions of specimen preparation. A possible explanation for our finding is that vesicles in horizontal cell

processes are few in number and do not congregate preferentially against the cell surface; thus, the chances of stabilizing with the fixative fluid the transient phenomenon of vesicle interaction with the plasmalemma are scanty indeed when the number of events occurring at any given time is very small.

Since the presynaptic zone is not visible at the surface of the horizontal cell processes, it is difficult to predict the significance of their membrane specializations. It is reasonable to assume that the symmetrical junction between the horizontal cell dendrites in pedicle invaginating synapses does not play a primary role in the functional interactions at the invaginating synapses, for it is also found elsewhere in the outer plexiform layer, at some distance from the photoreceptor endings, This leaves the A-face particle aggregates in both photoreceptor and horizontal cell membranes and the array of synaptic vesicle sites on the slopes of the photoreceptor ridge to account for the site of interaction between photoreceptors and horizontal cells. This set of morphological features, also found in the neuromuscular junction (13, 17, 41), may define the photoreceptor-to-horizontal cell contact. A reciprocal, horizontal-to-photoreceptor cell contact may correspond to the unspecialized region at the interface between horizontal cell processes and photoreceptor endings, as seen in inhibitory synapses of the central nervous system (25, 26). Alternatively, the symmetrical aggregates of A-face particles in the photoreceptor and horizontal cell membranes may subserve both pre- and postsynaptic functions, i.e. mediate the entry of calcium ions required for triggering transmitter release (22) and the mechanisms governing postsynaptic changes in membrane permeability.

In pedicle invaginating synapses, the presence of an A-face particle aggregate within the membrane of the horizontal cell dendrites opposite the tip of the invaginating midget bipolar dendrite strongly suggests that horizontal cells may be presynaptic to invaginating midget bipolars. Midget bipolars, then, would be the only variety of bipolar directly driven by horizontal cells, since no specialization exists at the interface between axonal endings of horizontal cells and rod bipolar dendrites in spherule invaginating synapses. Flat midget and diffuse cone bipolars, on the other hand, are not contacted by horizontal cells.

Bipolar Cell Dendrites

The problem of the synaptic connections of the invaginating bipolars is very intriguing. Invaginating midget and rod bipolar dendrites have similar membrane structure, for both lack particle aggregates at the invaginating synapse. However, their synaptic connections must be different, for invaginating midget bipolars receive a specialized contact from horizontal cells, whereas rod bipolars do not. Two alternative patterns of connections are consistent with this finding: either invaginating midget bipolars are driven by horizontal cells and rod bipolars by rods, or both varieties of bipolars are driven by the photoreceptors, but only the invaginating midget receives an additional input from the horizontal cells.

The basal contacts of cone pedicles resemble one type of synapse of the central nervous system (25, 26, 44) having a sparse complement of A-face particles in the pedicle membrane and a prominent cluster of B-face particles in the membrane of the bipolar dendrites. Therefore, the freeze-fracture profile strongly supports the argument that these contacts are synaptic in nature (12, 29). However, the crucial evidence is missing, for synaptic vesicle sites are not seen on the basal surface of cone pedicles. As previously suggested for horizontal cell processes, vesicle exocytosis may be such a rare event that the chances of stabilizing it by fixation may be very slim. Although we were unable to distinguish the basal contacts belonging to flat midget bipolars from those made by diffuse cone bipolars, there is no indication that they differ from each other with respect to their membrane organization. Therefore, diffuse and flat midget bipolars connect to a different number of cone cells (23), but they are likely to be influenced by the photoreceptors through the same physiological type of synapse.

The striking difference in membrane structure between the dendrites of the invaginating bipolars and those of the flat midget and diffuse cone bipolars is strongly suggestive of a functional diversity. Physiological studies in nonmammalian retinas have demonstrated that two functional varieties of bipolars exist, one hyperpolarizing, the other depolarizing upon light stimulation of the photoreceptors in the center of their receptive field; in both varieties, the response is antagonized by stimulation of distant photoreceptors (18, 20, 33, 46, 53). With respect to their lack of intramembrane specialization, the dendrites of the invaginating bipolars resemble the postsynaptic element of inhibitory synapses of the central nervous system (25, 26), whereas flat midget and diffuse cone bipolar dendrites have an intramembrane B-face particle aggregate, and thus resemble the postsyn-

aptic element of excitatory synapses (25, 26). An obvious implication of this resemblance is that invaginating bipolars may behave as the depolarizing bipolars of nonmammalian retinas, that is elements which hyperpolarize in the dark upon transmitter release by photoreceptors. Flat midget and diffuse bipolars, on the other hand, may behave as hyperpolarizing bipolars, that is elements which depolarize in the dark. A major objection, however, can be raised to this attractive interpretation: although invaginating midget and rod bipolar dendrites seem to receive different synaptic inputs, their membrane is equally unspecialized. Perhaps both invaginating midget and rod bipolars are depolarizing bipolars, but the midget bipolars are driven by horizontal cells, and the rod bipolars by rods. Alternatively, the absence of intramembrane specialization has no correlation with the bipolar response, but represents the result of the special geometry of the invaginating synapse. Particles within the membrane of the invaginating bipolars do not form aggregates, because loss of transmitter by diffusion is negligible in the confined extracellular environment of the synaptic invagination, and a sparse population of receptor sites may be adequate to trigger postsynaptic changes in membrane permeability. This being so, only invaginating midget bipolars may behave as depolarizing elements, for they receive a morphologically distinct input from horizontal cells.

Specialized Junctions between Horizontal and Bipolar Cells

Horizontal cells are connected to each other by a novel type of intercellular junction, characterized by: (*a*) symmetrical arrays of B-face particles arranged in parallel rows within the junctional membranes; (*b*) fluffy cytoplasmic material on the inner aspect of the plasmalemma; and (*c*) an enlarged intercellular cleft, traversed by cross bridges and bisected by a median plate. This junction connects: (*a*) the horizontal cell dendrites within the invaginating synapse; (*b*) unidentified horizontal cell processes in the neuropil of the outer plexiform layer beneath cone pedicles; and (*c*) possibly the axonal endings of the horizontal cells which penetrate the synaptic invagination of rod spherules. In spite of the fact that in thin-sectioned specimens this junction vaguely resembles a desmosome, its freeze-fracture appearance is totally different. The argument that interneuronal desmosomes may display a unique intramembrane organization is apparently invalid: in fact, at the neck of the synaptic invagination a junction between two processes both from the same cone pedicle has a freeze-fracture appearance identical to that of desmosomes in squamous epithelia (28). Although we cannot exclude that the junctions between horizontal cells may also provide mechanical adhesion, it is difficult to explain why this attachment device is only present between horizontal cells. It is interesting to note that the horizontal-to-horizontal cell junctions are clearly different from, but may coexist with, gap junctions. Further studies on serial-sectioned specimens are necessary to establish the precise connectivity of the horizontal cells whose processes interact at the junctions scattered throughout the neuropil underlying the cone pedicles. However, it seems particularly relevant that dendrites of different horizonal cells, which synapse with the same pedicle synaptic ridge, and possibly, axonal endings of different horizontal cells, which synapse with a single rod spherule, are connected to each other by this unusual type of intercellular junction. At present, it is difficult to conceive of a type of influence, different from electrical coupling and conventional synaptic interactions, exchanged by neurons which are connected to a single presynaptic element. Nevertheless, it may not be merely fortuitous that vesicles are occasionally found in the horizontal cell cytoplasm at a short distance from the junctional site.

Freeze-fracturing reveals the existence of a large number of minute gap junctions throughout the outer plexiform layer. Because of their small size they are difficult to identify in thin-sectioned specimens, and consequently they were undetected by previous investigators of the primate retina. Gap junctions are present between horizontal cells; other gap junctions may interconnect the bipolar dendrites that synapse with each cone pedicle. In nonmammalian retinas, it has been repeatedly demonstrated that horizontal cells are electrically coupled (19, 32, 47); with the electron microscope, junctions characterized by close surface apposition, probably gap junctions, have been observed between horizontal cell processes in a variety of vertebrate species (cf. reference 50). Thus, also in primates, horizontal cells are likely to be electrically coupled. On the other hand, no physiological information is available on the presence of low-resistance connections between bipolar cells. With respect to the process of encoding visual informa-

tion, the precise significance of the minute gap junctions between primate horizontal and bipolar cells is unclear; however, the ubiquitous presence of gap junctions in the retina seems to strengthen further the concept (43) that the synaptic interplay between the retinal neurons is more crucial to visual discrimination than their spatial segregation into a multitude of independent channels.

It is important to note that the majority of the junctional specializations which occur in the outer plexiform layer of the primate retina is also found in the rabbit and may therefore be typical of the mammalian retina in general.

We wish to thank Dr. T. N. Wiesel for many stimulating discussions.

This investigation was supported in part by United States Public Health Service grant EY 01344-01.

Received for publication 9 October 1974, and in revised form 23 December 1974.

REFERENCES

1. AKERT, K., K. PFENNINGER, C. SANDRI, and H. MOORE. 1972. Freeze etching and cytochemistry of vesicles and membrane complexes in synapses of the central nervous system. *In* Structure and Function of Synapses. G. D. Pappas and D. P. Purpura, editors. Raven Press, New York, 67–86.
2. BAYLOR, D. A., M. G. F. FUORTES, and P. M. O'BRYAN. 1971. Receptive fields of cones in the retina of the turtle. *J. Physiol.* **214**:265–294.
3. BIRKS, R., H. E. HUXLEY, and B. KATZ. 1960. The fine structure of the neuromuscular junction of the frog. *J. Physiol.* **150**:134–144.
4. BOYCOTT, B. B., and J. E. DOWLING. 1969. Organization of the primate retina: light microscopy. *Philos. Trans. R. Soc. Lond. Ser. B Biol. Sci.* **255**:109–184.
5. BOYCOTT, B. B., and H. KOLB. 1973. The horizontal cells of the rhesus monkey retina. *J. Comp. Neurol.* **148**:115–140.
6. BRANTON, D. 1966. Fracture faces of frozen membranes. *Proc. Natl. Acad. Sci. U. S. A.* **55**:1048–1056.
7. BUNT, A. H. 1971. Enzymatic digestion of synaptic ribbons in amphibian retinal photoreceptors. *Brain Res.* **25**:571–577.
8. CARTAUD, J., E. L. BENEDETTI, J. B. COHEN, J.-C. MEUNIER, and J.-P. CHANGEUX. 1973. Presence of a lattice structure in membrane fragments rich in nicotinic receptor protein from the electric organ of *Torpedo marmorata*. *FEBS (Fed. Eur. Biochem. Soc.) Lett.* **33**:110–113.
9. COUTEAUX, R., and M. PÉCOT-DECHAVASSINE. 1970. Vésicules synaptiques et poches au niveau des "zones actives" de la jonction neuromusculaire. *C. R. Hebd. Séances Acad. Sci. Sér. D Sci. Nat.* **271**:2346–2349.
10. DEL CASTILLO, J., and B. KATZ. La base "quantale" de la transmission neuro-musculaire. *In* Microphysiologie comparée des éléments excitables. Coll. Int. C.N.R.S. Paris **67**:245–254.
11. DICKINSON, A. H., and T. S. REESE. 1974. Freeze-fractured synapses in stimulated and unstimulated frog sympathetic ganglia. *Anat. Rec.* **178**:344–345. (Abstr.).
12. DOWLING, J. E., and B. B. BOYCOTT. 1966. Organization of the primate retina: electron microscopy. *Proc. R. Soc. Lond. Ser. B Biol. Sci.* **166**:80–111.
13. DREYER, F., K. PEPER, K. AKERT, C. SANDRI, and H. MOOR. 1973. Ultrastructure of the "active zone" in the frog neuromuscular junction. *Brain Res.* **62**:373–380.
14. FUORTES, M. G. F., E. A. SCHWARTZ, and E. J. SIMON. 1973. Colour-dependence of cone responses in the turtle retina. *J. Physiol.* **234**:199–216.
15. GRAY, E. G., and H. L. PEASE. 1971. On understanding the organization of the retinal receptor synapses. *Brain Res.* **35**:1–15.
16. HEUSER, J. E., and T. S. REESE. 1973. Evidence for recycling of synaptic vesicle membrane during transmitter release at the frog neuromuscular junction. *J. Cell Biol.* **57**:315–344.
17. HEUSER, J. E., T. S. REESE, and D. M. D. LANDIS. 1974. Functional changes in frog neuromuscular junctions studied with freeze-fracture. *J. Neurocytol.* **3**:109–131.
18. KANEKO, A. 1970. Physiological and morphological identification of horizontal, bipolar and amacrine cells in goldfish retina. *J. Physiol.* **207**:623–633.
19. KANEKO, A. 1971. Electrical connexions between horizontal cells in the dogfish retina. *J. Physiol.* **213**:95–105.
20. KANEKO, A. 1973. Receptive field organization of bipolar and amacrine cells in the goldfish retina. *J. Physiol.* **235**:133–153.
21. KARNOVSKY, M. J. 1967. The ultrastructural basis of capillary permeability studied with peroxidase as a tracer. *J. Cell Biol.* **35**:213–236.
22. KATZ, B. 1969. The Release of Neural Transmitter Substances. Liverpool University Press, Liverpool.
23. KOLB, H. 1970. Organization of the outer plexiform layer of the primate retina: electron microscopy of Golgi-impregnated cells. *Philos. Trans. R. Soc. Lond. Ser. B Biol. Sci.* **258**:261–283.
24. LADMAN, A. J. 1958. The fine structure of the rod-bipolar cell synapse in the retina of the albino rat. *J. Biophys. Biochem. Cytol.* **4**:459–466.
25. LANDIS, D. M. D., and T. S. REESE. 1974. Differences in membrane structure between excitatory and inhibitory synapses in the cerebellar cortex. *J. Comp. Neurol.* **155**:93–126.
26. LANDIS, D. M. D., T. S. REESE, and E. RAVIOLA.

1974. Differences in membrane structure between excitatory and inhibitory components of the reciprocal synapse in the olfactory bulb. *J. Comp. Neurol.* **155**:67–92.

27. LASANSKY, A. 1971. Synaptic organization of cone cells in the turtle retina. *Philos. Trans. R. Soc. Lond. Ser. B Biol. Sci.* **262**:365–381.
28. MCNUTT, N. S., and R. S. WEINSTEIN. 1973. Membrane ultrastructure at mammalian intercellular junctions. *Prog. Biophys. Mol. Biol.* **26**:47–101.
29. MISSOTTEN, L. 1965. The Ultrastructure of the Human Retina. Editions Arscia Uitgaven, Brussels.
30. MISSOTTEN, L., M. APPELMANS, and J. MICHIELS. 1963. L'ultrastructure des synapses des cellules visuelles de la rétine humaine. Bull. Mém. Soc. Fr. Ophthalmol. **76**:59–82.
31. MOOR, H., K. MÜHLETHALER, H. WALDNER, and A. FREY-WYSSLING. 1961. A new freezing-ultramicrotome. *J. Biophys. Biochem. Cytol.* **10**:1–14.
32. NAKA, K. I., and W. A. H. RUSHTON. 1967. The generation and spread of S-potentials in fish (Cyprinidae). *J. Physiol.* **192**:437–461.
33. NELSON, R. 1973. A comparison of electrical properties of neurons in *Necturus* retina. *J. Neurophysiol.* **36**:519–535.
34. NICKEL, E., and L. T. POTTER. 1973. Ultrastructure of isolated membranes of *Torpedo* electric tissue. *Brain Res.* **57**:508–517.
35. O'BRYAN, P. M. 1973. Properties of the depolarizing synaptic potential evoked by peripheral illumination in cones of the turtle retina. *J. Physiol.* **235**:207–223.
36. PERRI, V., O. SACCHI, E. RAVIOLA, and G. RAVIOLA. 1972. Evaluation of the number and distribution of synaptic vesicles at cholinergic nerve-endings after sustained stimulation. *Brain Res.* **39**:526–529.
37. PFENNINGER, K., K. AKERT, H. MOOR, and C. SANDRI. 1972. The fine structure of freeze-fractured presynaptic membranes. *J. Neurocytol.* **1**:129–149.
38. PFENNINGER, K. H., and C. M. ROVAINEN. 1974. Stimulation- and calcium-dependence of vesicle attachment sites in the presynaptic membrane; a freeze-cleave study on the lamprey spinal cord. *Brain Res.* **72**:1–23.
39. PINTO DA SILVA, P., and D. BRANTON. 1970. Membrane splitting in freeze-etching. Covalently bound ferritin as a membrane marker. *J. Cell Biol.* **45**:598–605.
40. POLYAK, S. L. 1941. The Retina. The University of Chicago Press, Chicago.
41. RASH, J. E., M. H. ELLISMAN, and L. A. STAEHELIN. 1973. Freeze-cleaved neuromuscular junctions: macromolecular architecture of post-synaptic membranes of normal vs. denervated muscle. *J. Cell Biol.* **59**(2, Pt. 2):280, a. (Abstr.).
42. RAVIOLA, E., and N. B. GILULA. 1973. Membrane particle aggregates at specialized contacts between cone, bipolar and horizontal cells in the monkey retina. *J. Cell Biol.* **59**(2, Pt. 2):282 a. (Abstr.).
43. RAVIOLA, E., and N. B. GILULA. 1973. Gap junctions between photoreceptor cells in the vertebrate retina. *Proc. Natl. Acad. Sci. U. S. A.* **70**:1677–1681.
44. SANDRI, C., K. AKERT, R. B. LIVINGSTON, and H. MOOR. 1972. Particle aggregations at specialized sites in freeze-etched postsynaptic membranes. *Brain Res.* **41**:1–16.
45. SATIR, B., C. SCHOOLEY, and P. SATIR. 1973. Membrane fusion in a model system. Mucocyst secretion in *Tetrahymena*. *J. Cell Biol.* **56**:153–176.
46. SCHWARTZ, E. A. 1974. Responses of bipolar cells in the retina of the turtle. *J. Physiol.* **236**:211–224.
47. SIMON, E. J. 1973. Two types of luminosity horizontal cells in the retina of the turtle. *J. Physiol.* **230**:199–211.
48. SJÖSTRAND, F. S. 1953. The ultrastructure of the retinal rod synapses of the guinea pig eye. *J. Appl. Phys.* **24**:1422.
49. SJÖSTRAND, F. S. 1974. A search for the circuitry of directional selectivity and neural adaptation through three-dimensional analysis of the outer plexiform layer of the rabbit retina. *J. Ultrastruct. Res.* **49**:60–156.
50. STELL, W. K. 1972. The morphological organization of the vertebrate retina. *In* Physiology of Photoreceptor Organs. M. G. F. Fuortes, *editor*. Handbook of Sensory Physiology. Vol. VII. No. 2. Springer-Verlag Gmbh., Berlin. 111–213.
51. STREIT, P., K. AKERT, C. SANDRI, R. B. LIVINGSTON, and H. MOOR. 1972. Dynamic ultrastructure of presynaptic membranes at nerve terminals in the spinal cord of rats. Anesthetized and unanesthetized preparations compared. *Brain Res.* **48**:11–26.
52. TILLACK, T. W., and V. T. MARCHESI. 1970. Demonstrations of the outer surface of freeze-etched red blood cell membranes. *J. Cell Biol.* **45**:649–653.
53. WERBLIN, F. S., and J. E. DOWLING. 1969. Organization of the retina of the mudpuppy, *Necturus maculosus*. II. Intracellular recording. *J. Neurophysiol.* **32**:339–355.